NATIONAL ADVISORY COMMITTEE FOR AERONAUTICS

TECHNICAL NOTE

No. 938

THE INWARD BULGE TYPE BUCKLING OF MONOCOQUE CYLINDERS I - CALCULATION OF THE EFFECT UPON THE BUCKLING STRESS OF A COMPRESSIVE FORCE, A NONLINEAR DIRECT STRESS DISTRIBUTION, AND A SHEAR FORCE

By N. J. Hoff and Bertram Klein
Polytechnic Institute of Brooklyn

Washington
October 1944

NATIONAL ADVISORY COMMITTEE FOR AERONAUTICS

TECHNICAL NOTE NO. 938

THE INWARD BULGE TYPE BUCKLING OF MONOCOQUE CYLINDERS

I - CALCULATION OF THE EFFECT UPON THE BUCKLING STRESS OF A COMPRESSIVE FORCE, A NONLINEAR DIRECT STRESS DISTRIBUTION, AND A SHEAR FORCE

By N. J. Hoff and Bertram Klein

SUMMARY

In the present part I of a series of reports on the inward bulge type buckling of monocoque cylinders the buckling load in combined bending and compression is first derived. Next the reduction in the buckling load because of a nonlinear direct stress distribution is determined. In experiments nonlinearity may result from an inadequate stiffness of the end attachments, in actual airplanes from the existence of concentrated loads or cut-outs. The effect of a shearing force upon the critical load is investigated through an analysis of the results of tests carried out at GALCIT with 55 reinforced monocoque cylinders. Finally a simple criterion of general instability is presented in the form of a buckling inequality which should be helpful to the designer of a monocoque in determining the sizes of the rings required for excluding the possibility of inward bulge type buckling.

INTRODUCTION

Large monocoque fuselages reinforced by closely spaced stringers and rings are likely to buckle, when loaded, according to a pattern which involves simultaneous distortions of the stringers, the rings, and the sheet covering. This type of buckling is known as general instability. The details of the pattern vary with

the loading. When the maximum stress in the fuselage is caused mainly by a bending moment, which may be accompanied by a small shear force, compressive force, or torque, the characteristic feature of the distorted shape is an inward bulge extending symmetrically from the stringer that is most highly stressed in compression. (See fig. 1.) In some cases there is a single inward bulge; in others several appear along the most highly stressed compressive stringer, and these may occur when the bending moment is constant over a uniform portion of considerable length of a monocoque cylinder. Often a few shallower secondary bulges appear alongside the main bulges, but in all the cases so far observed the distortions are restricted to the neighborhood of the stringer most highly stressed in compression. This type of general instability is denoted as inward bulge type buckling.

Calculations of the critical load corresponding to the inward bulge type buckling were first published by Hoff in 1938 in reference 1, in which a single experiment was also described. The derivation of the critical load was accomplished with the aid of the Rayleigh-Ritz-Timoshenko method, and the strain energy stored in the sheet covering was neglected. The first extensive series of tests was carried out at GALCIT and was reported in reference 2. Comparison of the test results with the theory of reference 1 showed great discrepancies, and the use of a semi-empirical formula was suggested. In reference 3 Hoff revised his theory in the light of this new experimental evidence. The following are the basic ideas of the revised theory:

The strain energy stored in the sheet covering is negligibly small, and the shapes of the deflections of the rings and the stringers are governed by the least work requirement regardless of the strain energy stored in the sheet. The size of the bulge in the circumferential direction, however, is governed by the state of the sheet. The bulge extends only to regions where the shear rigidity of the panels is reduced because of the buckling of the sheet between the rings and the stringers. The circumferential length of the bulge is characterized by the parameter n which is the ratio of π to the angle φ_0 measured (in radians) from the stringer which is most highly stressed in compression to the stringer where the deformation of the ring ends. As a rule, n is greater than 2, since the bulge is not likely to extend to the tension side of the monocoque cylinder.

There is no theory available, however, by which the actual value of n could be determined. In reference 3 it was suggested that a chart developed from the data of the GALCIT experiments be used for this purpose.

The object of the present investigations is to improve upon the theory of references 1 and 3. It is believed that the crucial point in the development of a rigorous and reliable theory is an understanding of the action of the sheet covering. As a contribution toward this understanding the effect of a compressive load upon the critical stress of general instability in a bent monocoque cylinder is calculated in the third section of this report. In the formula developed, the parameter n appears. It is hoped that an experimental investigation, to be reported in part II of the present series dealing with the inward bulge type buckling, will throw some light upon the variation of n with the compressive load. Since n depends mainly on the state of the sheet covering, and this state is materially influenced by the compressive force, knowledge of the functional connection between n and the compressive force may be helpful in clarifying the role of the sheet in general instability.

The fifth section of this report presents a detailed analysis, in the light of the theory of reference 3, of the experimental results obtained at GALCIT with 55 reinforced monocoque cylinders tested in combined bending and shear and described in reference 4. The main purpose of the analysis is to investigate the effect of a shear force upon the value of the parameter n. Simultaneously a convenient semigraphic method of analyzing data of this kind is developed and presented.

The fourth and sixth sections present incidental results of the investigations. The theory developed in the former became necessary because it was observed that an accurate linear direct stress distribution in a bent monocoque cylinder is not easily obtained in experiment. Consequently the effect of a deviation from linearity had to be calculated. In the sixth section an inequality is developed which permits a quick approximate determination as to whether a monocoque cylinder is liable to fail in general instability.

The seventh and eighth sections compare theory with experiment. The ninth section contains the conclusions.

This investigation, conducted at the Polytechnic Institute of Brooklyn, was sponsored by, and conducted with financial assistance from, the National Advisory Committee for Aeronautics.

SYMBOLS

A	cross-sectional area of a stringer
d	stringer spacing measured along the circumference
E_r	Young's modulus for the material of the ring
E_{str}	Young's modulus for the material of the stringer
h	height of center of gravity of stringer cross section measured perpendicularly from its base
$I_{cu\ sh}$	moment of inertia of the curved sheet taken about its centroidal axis
I_r	moment of inertia of ring section and its effective width of sheet for bending in the radial direction
$I_{r\ o}$	moment of inertia of ring section without its effective sheet for bending in the radial direction
I_{str}	$I_{str\ r} + (5/8)(1/n^2)\ I_{str\ t}$
$I_{str\ o}$	moment of inertia of stringer cross section without its effective sheet for bending in the radial direction
$I_{str\ r}$	moment of inertia of stringer cross section and its effective width of sheet for bending in the radial direction
$I_{str\ t}$	moment of inertia of stringer cross section with its effective sheet for bending in the tangential direction
I_{xx}	$I_{str\ o}$

I_{yy} moment of inertia of stringer cross section without its effective sheet for bending in the tangential direction

k_1 proportionality factor in the expression for the buckling of a circular cylinder loaded with uniform axial compression

k_2 proportionality factor in the expression for the buckling of a flat rectangular plate loaded with uniform axial compression

L total length of wave in the axial direction

L_1 distance between the rings measured axially along the cylinder

m number of rings included in the length L

M_1, M_2, M_3, M_4 functions of the parameter n associated with the determination of the strain energies stored in the rings and the stringers, and the external work

n a parameter characterizing the shape of the ring deflection which is equal to the ratio of the total circumference to that cut off by the buckling pattern, or π/φ_0

P_{cr} load carried by the most highly compressed stringer and its effective width of sheet at buckling in pure bending

$P_{cr\ gi}$ P_{cr} when pattern is general instability

$P_{cr\ p}$ P_{cr} when pattern is panel instability

$P_{cr\ tot}$ load carried by the most highly compressed stringer and its effective width of sheet at buckling in bending and compression

r the radius of the circular cylinder

R a function of n similar to those denoted by M_1, M_2, and so forth

S total number of stringers in the structure

t the thickness of the sheet covering

U_r the strain energy stored in the rings

U_{str} the strain energy stored in the stringers

$2w_{cu}$ effective width of curved sheet

w_r radial displacement of a point on a ring or a stringer

w_t tangential displacement of a point on a ring or a stringer

W work done by external load

x coordinate measuring distance along the axis of the cylinder

$\overline{y}$ the distance between the centroidal axes of the stringer cross section alone and of the combined stringer cross section and its effective curved sheet

2α maximum deflection of the most compressed stringer of the most highly deflected ring

γ factor in the formula for the critical strain for pure bending

ΔL change in the distance between $x = 0$ and $x = L$ due to distortions

Δy_c shift in the center of gravity of the effective sheet due to its curvature

ϵ strain at the edge of a panel

ϵ_{max} strain in the most compressed stringer at failure

θ an angular measure

λ equivalent length factor defined by equation (40)

Λ buckling index defined by equation (39)

Λ_o reduced buckling index where effective width of sheet and tangential moment of inertia of stringer cross section are neglected

ν compressive load divided by perimeter

ξ factor similar to γ

φ an angular measure

φ_o angle defining end of the circumferential wave

CALCULATION OF THE BUCKLING LOAD IN COMBINED COMPRESSION AND BENDING

If upon a reinforced monocoque cylinder a compressive load is acting which is not sufficient to cause buckling by itself, and a slowly increasing pure bending moment is applied, failure may occur in the form of the inward bulge type general instability. The calculation of the corresponding critical load can be carried out in exactly the same manner as was done in references 1 and 3 for the case of pure bending alone. The buckled shape is assumed to satisfy the equations

$$w_r = -(\alpha/2)[1-\cos(2\pi x/L)][\cos(n\varphi) + \cos(2n\varphi)] \quad (1)$$

$$w_t = (\alpha/2)[1-\cos(2\pi x/L)][(1/n)\sin(n\varphi) + (1/2n)\sin(2n\varphi)] \quad (2)$$

provided that

$$\varphi \leq \varphi_o \quad (3)$$

where

$$n = \pi/\varphi_o \quad (4)$$

and

w_r radial displacement

w_t tangential displacement

α an indetermined parameter

x coordinate measured along the axis of the cylinder

L full wave length in axial direction

φ coordinate in the circumferential direction

φ_o half wave length (in radians) in the circumferential direction

Equations (1) and (2) are identical with equations (62) and (63) of reference 1. The deflected shape is shown in figures 1 to 3 which correspond to figures 13 to 15 of reference 1, and to figures 3 to 5 of reference 3.

The critical value of the bending moment is reached when the work done by the direct stress, linearly distributed over the cross sections at $x = 0$ and $x = L$, is equal to the strain energy stored in the rings and the longitudinals. The strain energy is caused by the deflections w_r and w_t; while the work is the product of the afore-mentioned direct stresses by the relative displacements of their points of application corresponding to the assumed pattern of distortions. In this buckling condition the strain energy terms do not change because of the added uniform compression. They are quoted here from reference 1 with some changes in the notation. The strain energy U_r stored in the rings is

$$U_r = (3\pi/16)\,\alpha^2\, M_2(m + 1)(1/r)^3 E_r I_r \tag{5}$$

where

$$M_2 = 17n^3 - 10n + (2/n) \tag{6}$$

and m is the number of rings that distort at buckling, r the radius of the cylinders, and $E_r I_r$ the bending rigidity of a ring and the effective width of sheet attached to it. Equation (5) corresponds to equation (65) of reference 1, equation (6) to equation (80a) in reference 1, and in a substitution use was made of the first of equations (11) in reference 3. Equation (5) is valid only if m is an integer greater than unity. The strain energy U_{str} stored in the stringers is

$$U_{str} = 2\pi^5 \alpha^2 M_3 (r/d)(1/L^3) E_{str} I_{str} \tag{7}$$

where

$$M_3 = (1/n) \tag{8}$$

$$I_{str} = I_{str\ r} + (5/8)(1/n^2)I_{str\ t} \qquad (9)$$

and

d distance between adjacent stringers measured along the circumference

E_{str} Young's modulus for the material of the stringer

$I_{str\ r}$ and $I_{str\ t}$ moments of inertia of the stringer section for bending radially and tangentially, respectively, both calculated with due consideration of the effective width of sheet

Equations (7), (8), and (9) correspond to equations (70), (80a), and (70a) of reference 1.

In the development of the expression for the work W done by the applied loads the procedure of section 18(c) of reference 1 can be followed. If ν denotes the uniformly distributed compressive load applied to a unit length of the perimeter of the cylinder, the total load acting upon an infinitesimal length $rd\varphi$ of the circumference because of the simultaneous application of compressive force and bending moment can be written, with consideration of equation (71) of reference 1, as

$$dP = (P/d)\cos\varphi\ rd\varphi + \nu\ rd\varphi \qquad (10)$$

The shortening of the distance between points $x = 0$ and $x = L$ lying on the same stringer is

$$\Delta L = (1/4)(\pi^2/L)\ \alpha^2[\cos(n\varphi) + \cos(2n\varphi)]^2$$

$$+ (1/4)(\pi^2/L)\ \alpha^2[(1/n)\sin(n\varphi) + (1/2n)\sin(2n\varphi)]^2 \qquad (11)$$

The total work done by the loads is, therefore,

$$W = \int_{-\pi/n}^{\pi/n} r\ \Delta L\ [(P/d)\cos\varphi + \nu]\ d\varphi$$

$$= (1/2)\pi^2\alpha^2(r/L)\left\{(P/d)(M_1+R_1) + \pi\nu[(1/n)+(5/8)(1/n^3)]\right\} \qquad (12)$$

where

$$M_1 = \sin(\pi/n)\left\{1 - [1/(1-n^2)] + [1/2(1-4n^2)] - [1/(1-9n^2)] + [1/2(1-16n^2)]\right\} \quad (13)$$

$$R_1 = (1/2n^2)\sin(\pi/n)\left\{(5/4) - [1/(1-n^2)] - [1/(1-4n^2)] + [1/(1-9n^2)] - [1/4(1-16n^2)]\right\} \quad (14)$$

Equation (12) differs from the sum of equations (76) and (78) of reference 1 only in the term containing ν, while equations (13) and (14) are identical with equations (76a) and (78a) of reference 1 (except for a printing error in the latter).

As stated before, the buckling condition is

$$W = U_r + U_{str} \quad (15)$$

The load P in the most highly stressed stringer on the compression side caused by bending alone will be denoted by P_{cr} if it satisfies equation (15). By writing P_{cr} for P in equation (12), by substituting the expressions of equations (5), (7), and (12) into equation (15), and by solving for P_{cr}, there is obtained

$$P_{cr} = [1/(M_1 + R_1)]\left\{(E_{str}I_{str}/AL_1^2)\left[(3/8\pi)M_2(m+1)^2 + 4\pi^3 M_3 A/(m+1)^2\right] - \pi\nu\, dM_4\right\} \quad (16)$$

In this equation

$$A = (r^4/L_1^3 d)(E_{str}I_{str}/E_r I_r) \quad (17)$$

is the nondimensional buckling index originally defined in equation (86) of reference 1. Moreover, L_1 is the distance between adjacent rings, and consequently

$$L = (m + 1) L_1 \tag{18}$$

Also,

$$M_4 = (1/n) + (5/8)(1/n^3) \tag{19}$$

The number m of rings involved in buckling is determined from the requirement that P_{cr} must be a minimum. Consequently the differential coefficient of P_{cr} with respect to m must vanish. Equation (16) may be represented by the equation

$$P_{cr} = A \left\{ a(m + 1)^2 + [b/(m + 1)^2] - B \right\} \tag{a}$$

Differentiating with respect to $(m + 1)^2$ rather than to m, and equating the differential coefficient to zero results in

$$(m + 1)^4 = (b/a) \tag{b}$$

Substitution into equation (a) yields

$$P_{cr} = A [2(ab)^{1/2} - B] \tag{c}$$

With the actual expressions instead of the symbols a, b, A, and B, there is obtained

$$P_{cr} = \sqrt{6}\, \pi\, (1/L_1^2 A^{1/2})\, [(M_2 M_3)^{1/2}/(M_1 + R_1)]\, E_{str} I_{str} - \pi v d\, [M_4/(M_1 + R_1)] \tag{20}$$

It was shown in reference 3 (see equations (17) and (18)) that in very good approximation

$$(\pi/\sqrt{6})\, [(M_1 + R_1)/(M_2 M_3)^{1/2}] = (1/n^2) \tag{21}$$

With the aid of equation (21) it can be shown that in

good approximation

$$\pi M_4/(H_1 + R_1) = 1 + (0.9/n^2) \qquad (22)$$

After several transformations and with the aid of equations (21) and (22), equation (20) can be written in the form

$$P_{cr} = n^2\sqrt{\frac{d}{L_1}}\frac{\pi^2\sqrt{E_{str}I_{str}E_rI_r}}{r^2} - \left(1 + \frac{0.9}{n^2}\right)\nu d \qquad (23)$$

This equation differs from equation (20) of reference 3 only in the term containing ν. It must be remembered, however, that in it P_{cr} denotes the compressive force caused by bending alone in the most highly stressed stringer on the compression side. If the total load $P_{cr\ tot}$ caused by bending and compression is required, νd must be added to the value of P_{cr}. Consequently,

$$P_{cr\ tot} = n^2\sqrt{\frac{d}{L_1}}\frac{\pi^2\sqrt{E_{str}I_{str}E_rI_r}}{r^2} - \frac{0.9}{n^2}\nu d \qquad (24)$$

Since the value of n usually is equal to or greater than 3, it may be seen from equation (24) that the total load in the most highly stressed stringer in compression is little changed if part of it is caused by an external compressive load and part by an external bending moment, instead of being caused entirely by an external bending moment as in references 1 and 3. This statement is correct only if the value of n is not affected by the compressive load. However, if the compressive load decreases the shearing rigidity of the sheet, it is expected that n, and consequently $P_{cr\ tot}$, should decrease, as was pointed out in reference 3. Consequently an experimental investigation of the inward bulge type general instability in simultaneous bending and compression should contribute to the clarification of the effect of the sheet on the buckling load. Such an investigation is now being carried out in the Aircraft Structures Laboratory of the Polytechnic Institute of Brooklyn. Its results will form the contents of part II of this report.

THE EFFECT OF A NONLINEAR DIRECT STRESS DISTRIBUTION

The effect upon general instability of a nonlinear stress distribution over the cross section of the bent monocoque cylinder is investigated in this section. The investigation was undertaken because of the observation that an accurate linear stress distribution is not easily obtained in experiment. It is desirable, therefore, to establish, at least approximately, the possible deviations from the theoretical buckling load caused by nonlinearity. Moreover, it is likely that concentrated loads, cut-outs, and so forth may result in a nonlinear stress distribution in an actual airplane the effect of which might be a change in the load at which general instability would occur.

The probable maximum deviation can be easily determined on the assumption that the compressive stress is constant over the region of the inward bulge ($|\varphi| \leq \varphi_0$). In the calculation of the buckling load the strain energy terms remain unaltered, and are represented by equations (5) to (9). The work done by the external load can be recalculated upon replacing equation (10) by the equation

$$dP = (P/d)rd\varphi + vrd \tag{25}$$

The effect of this change is to have

$$\pi[(1/n) + (5/8)(1/n^3)] = \pi M_4$$

in place of $(M_1 + R_1)$ in equation 12. Consequently the critical load acting upon the stringers on the compression side may be obtained by multiplying the right-hand side of equation (23) by

$$(M_1 + R_1)/\pi M_4$$

Since according to equation (22) the preceding ratio is equal to

$$1/[1 + (0.9/n^2)]$$

the critical load becomes

$$P_{cr} = \frac{n^2}{1+(0.9/n^2)} \sqrt{\frac{d}{L_1}} \frac{\pi^2 \sqrt{E_{str} I_{str} E_r I_r}}{r^2} - \nu d \qquad (26)$$

Consequently the total buckling load - due to both bending and compression - is given by the equation

$$P_{cr\ tot} = \frac{n^2}{1+(0.9/n^2)} \sqrt{\frac{d}{L_1}} \frac{\pi^2 \sqrt{E_{str} I_{str} E_r I_r}}{r^2} \qquad (27)$$

In the case of pure bending ($\nu = 0$) equation (26) naturally reduces to equation (27). It may be seen that the deviation in the value of the critical load P_{cr} from that corresponding to a linear stress distribution is small. In most cases n not being less than 3 the factor $[1 + (0.9/n^2)]$ is not greater than 1.1. On the other hand, the change in the stress distribution may cause n to become smaller, in which case the decrease in the value of P_{cr} would be more pronounced.

Although from the preceding calculations it follows that a deviation from a linear stress distribution slightly decreases the maximum load in the most highly compressed stringer - that is, it decreases slightly the maximum compressive strain at buckling - at the same time the critical bending moment may even increase. With a linear stress distribution the bending moment is

$$M_{cr} = 2(P_{cr}/d)r^2 \int_0^{\pi} \cos^2\varphi \, d\varphi = \pi r^2 (P_{cr}/d) \qquad (28)$$

If the rather unreasonable assumption is made that the compressive stress is constant over one-half the cross section of the cylinder, and an equal constant tensile stress prevails over the other half, the bending moment becomes

$$M_{cr} = 4(P_{cr}/d)r^2 \int_0^{\pi/2} \cos\varphi \, d\varphi = 4r^2 (P_{cr}/d) \qquad (29)$$

Therefore, the quotient of the moments, for the same P_{cr},

is $4/\pi = 1.27$, while the quotient of the critical loads corresponding to constant and linear stress distribution, respectively, is 1.1. Hence the bending moment at buckling is increased in the ratio 1.16/1. With an assumption which restricts the constant stress to a smaller region, the increment in the value of the critical bending moment would be even smaller. Of course, stress distributions encountered in practice are always closer to linearity than the law assumed in the present calculations. Consequently it is reasonable to conclude that small deviations from linearity slightly reduce the buckling stress, but hardly change the buckling moment.

ANALYSIS OF THE RESULTS OF THE COMBINED BENDING AND SHEAR TESTS CARRIED OUT IN THE GUGGENHEIM AERONAUTIC LABORATORY OF THE CALIFORNIA INSTITUTE OF TECHNOLOGY

The Combined Bending and Shear Tests of GALCIT

Fifty-five reinforced monocoque cylinders were tested in combined bending and shear in the Guggenheim Aeronautic Laboratory of the California Institute of Technology. The results of the tests were published in reference 4, which also contains a report on eight additional cylinders of varying length tested in pure bending. In the present report all these test results are analyzed according to the theory developed in references 1 and 3. The main purpose of the analysis is to investigate the effect of shear upon the value of n, a parameter amply discussed in references 1 and 3 as well as in the preceding sections of this report. Simultaneously a convenient semigraphic method of analyzing data of this kind is developed and presented, and the effect of simplifying assumptions is investigated.

Figure 4 shows the monocoque cylinder and its details, together with part of the notation used in this report. The stringers are of elliptic cross section. Their cross-sectional area A is 0.0324 square inch. The greatest moment of inertia $I_{yy} = 0.000563$ inch^4, the smallest moment of inertia $I_{xx} = 0.000374$ inch^4. The cross section of the rings is rectangular, 0.366 by 0.0796 inch. Most of the cylinders are of 16-inch radius, the others of 10-inch radius. All are covered with sheet of 0.010-inch

thickness. The material is heat-treated aluminum alloy, presumably 17S-T. The ring spacing varies from 1 inch to 8 inches, the number of stringers from 10 to 40.

Effective Width of Sheet

In the calculation of the effective width $2w_{curved}$ of a curved panel loaded uniformly in compression Ebner's suggestion is followed here as in reference 3. Substitution of equations (24b) to (24d) into equation (24a) of reference 3 gives:

$$2w_{curved} = (1/\epsilon)(d/r)\left\{0.3t + 1.535\left[(t/d)(\epsilon r - 0.3t)r^{1/2}\right]^{2/3}\right\} \quad (30)$$

This is true as long as

$$2w_{curved} \leq d \quad (30a)$$

In this equation ϵ stands for the strain in the stringer at the edge of the panel. Since in the present analysis the effective width is calculated only in the most highly stressed region on the compression side, ϵ_{max} will be substituted for ϵ in all numerical calculations.

Equation (30) is approximate since the value of the numerical coefficients vary, in general, with the geometric and mechanical properties of the monocoque. Thus the factor 0.3 in the formula for the critical strain of the circular cylinder, equation (24d) of reference 3, may better be approximated by Donnell's formula (see sec. 22 of reference 1). Moreover, the value 3.62 assumed in the formula for the critical strain of a flat plate may deviate considerably from reality if the panels are short (the ring spacing L_1 is small) and if the stringers and rings provide much end restraint. In the general case equation (30) may be written in the form:

$$2w_{curved} = (1/\epsilon)(d/r)\left\{k_1 t + k_2^{1/3}\left[(t/d)(\epsilon r - k_1 t)r^{1/2}\right]^{2/3}\right\} \quad (31)$$

In this equation k_1 represents the numerical coefficient in the formula for the critical strain of the circular cylinder:

$$\epsilon_{curved} = k_1(t/r) \tag{32}$$

and k_2 the numerical coefficient in the formula for the critical strain of the flat rectangular panel:

$$\epsilon_{flat} = k_2(t/d)^2 \tag{33}$$

Figure 5a is a plot of $2w_{curved}$ against ϵ, calculated from equation (30) for the case $t = 0.01$ inch and $r = 10$ inches. The figure contains a family of curves representing the effective width for cylinders having different numbers S of stringers. Figure 5b differs from figure 5a only in that the radius of the cylinder $r = 16$ inches. The curves show that the effective width decreases monotonically with increasing strain, which is in agreement with expectation.

Moments of Inertia of Stringer and Effective Curved Sheet Combinations

(a) In the radial direction.- Since the effective sheet acting with the stringer is curved, its center of gravity lies a distance Δy_c above the point of intersection O of the median line of the curved sheet with the y axis. (See fig. 6.) This distance is given by the expression:

$$\Delta y_c = r - (1/2wt)r^2t\int_{-(w/r)}^{(w/r)} \cos\theta \, d\theta \tag{a}$$

where θ is measured counterclockwise from the axis y-y, as shown in the figure. If terms of higher order are neglected, evaluation of equation (a) yields the close approximation for the shift in the center of gravity of the sheet due to its curvature:

$$\Delta y_c = (2w)^2/(24r) \tag{b}$$

The location of the center of gravity of the combination of stringer and curved effective sheet now can be

determined. Taking moments about x-x, the horizontal axis through the center of gravity of the stringer alone, results in:

$$\bar{y} = (2wt)[h + (t/2) - \Delta y_c]/(A + 2wt) \qquad (c)$$

Here h is the distance from the x axis of the point of intersection of the bottom of the stringer with the y axis, and A is the cross-sectional area of the stringer.

The moment of inertia $I_{cu\ sh}$ of the curved sheet about its own centroidal axis is:

$$I_{cu\ sh} = r^3 t \int_{-(w/r)}^{(w/r)} (1 - \cos\theta)^2 d\theta - (2wt)(\Delta y_c)^2$$

$$= (4/5)(2wt)(\Delta y_c)^2 \qquad (d)$$

By the use of the parallel axis theorem the moment of inertia $I_{str\ r}$ of the combination about the centroidal axis through the common centroid can be calculated:

$$I_{str\ r} = I_{xx} + \bar{y}^2 A + (4/5)(\Delta y_c)^2(2wt)$$

$$+ [h + (t/2) - \Delta y_c - \bar{y}]^2(2wt) \qquad (e)$$

In this equation I_{xx} is the moment of inertia of the stringer cross section about its centroidal axis. With the aid of equations (b) and (c) equation (e) can be reduced to the form:

$$I_{str\ r} = I_{xx} + \frac{\left\{h + (t/2) - [(3w)^2/(24r)]\right\}^2}{(1/2wt) + (1/A)}$$

$$+ (4/5)[(2w)^2/(24r)]^2(2wt) \qquad (34)$$

Equation (34) is plotted in figure 7 for both cases $r = 10$ inches and $r = 16$ inches. The formula gives correct values for a flat sheet also if r is considered as

increasing beyond all bounds. A curve for this case is drawn for comparison. It shows that for large effective width neglecting the curvature may lead to definite deviations from equation (34).

(b) In the tangential direction.- The combined moment of inertia of effective curved sheet and stringer for bending about the vertical axis can also be calculated by simple integration. From figure 6:

$$\int_{-(w/r)}^{(w/r)} (r \sin \theta)^2 \, rtd\theta + I_{yy} \qquad (a)$$

where I_{yy} is the moment of inertia of the stringer section about the vertical axis. Evaluation of the integral yields the formula:

$$I_{str\ t} = I_{yy} + (1/2)tr^3[(2w/r) - \sin(2w/r)] \qquad (35)$$

For practical purposes it is permissible to expand the sine function in the bracket and to neglect all terms beyond the second. Thus equation (35) reduces to:

$$I_{str\ t} = I_{yy} + (1/12)(2w)^3 t \qquad (36)$$

It is understood that it is arbitrary to calculate the tangential moment of inertia, assuming the same effective width as that used in determining the radial moment of inertia. Although this procedure leads to unreasonably high values for $I_{str\ t}$ when $2w_{curved}$ is large, it is followed throughout this report, since no better approximation is known at present.

(c) Calculation of I_{str}.- In the analysis $I_{str\ t}$ always appears multiplied by $(5/8)(1/n^2)$. This value is plotted in figure 8 for $n = 3$. If n is different, the correct value can be obtained by multiplying by the factor $(3/n)^2$.

Equation (9) can now be graphed, plotting $2w_{curved}$ against I_{str} for both radii $r = 10$ inches and $r = 16$ inches taking $n = 3$. (See fig. 9.)

Effective Width of Sheet Acting with the Rings

In all calculations the effective width of sheet acting with the rings is assumed to be equal to 0.366 inch, the width of the ring. This arbitrary assumption is made since it does not appear likely that much of the curved sheet would follow the deflection pattern of the ring. If it flattens and bends about its own centroidal axis, much less strain energy is stored in it than if it bends about the common centroid of the ring and sheet combination. The actual deflection pattern, of course, corresponds to the least possible strain energy.

The One-Quarter Power Law

It was shown in reference 3 that the buckling index Λ (given in equation (17) of this report) is connected by a quarter-power law with the equivalent length factor λ, which is implicitly defined by the equation

$$P_{cr} = \pi^2 E_{str} I_{str} / (\lambda L_1)^2 \tag{37}$$

The quarter-power law is

$$\lambda = (1/n)\, \Lambda^{1/4} \tag{38}$$

In the computations Young's modulus was taken equal for all the materials of the cylinder. The simplified form of equation (17) is:

$$\Lambda_n = (r^4 / L_1^3 d)(I_{str\ n} / I_r) \tag{39}$$

where the subscript n signifies that I_{str}, and consequently Λ, depends upon the choice of the parameter n. Equation 39 is graphed in figures 10a and 10b for r = 10 inches and 16 inches, respectively, and for different numbers of stringers.

Transformation of equation (37) gives for λ:

$$\lambda_n = (\pi / L_1) \left[(1/\epsilon_{max}) I_{str\ n} / (A + 2wt) \right]^{1/2} \tag{40}$$

This equation is represented by the curves of figures 11a and 11b for $r = 10$ inches and $r = 16$ inches, respectively, and for different numbers of stringers. These graphs and equation (40) are useful in calculating the theoretical value of the equivalent length factor λ if ϵ_{max} is known from experiment.

From equations (39) and (40) Λ and λ were calculated on the assumption $n = 3$ for the 63 specimens investigated in this report. The logarithms of λ are plotted against the logarithms of Λ in figure 12 together with the theoretical straight line representing equation (38) for $n = 3$. The points in this graph are grouped and labeled according to the number of stringers and the ring spacing of the test specimens. For instance, (12,4) refers to specimens having 12 stringers, and rings spaced 4 inches apart. The numbers written next to the points represent values of n calculated according to the procedure explained later.

It may be seen that for a given radius and for a given number of stringers S all experimental points lie about a straight line parallel to the theoretical one. This indicates that the actual value of n is approximately constant and independent of the ring spacing. On the other hand, there is a marked increase in the actual value of n with increasing S. It was this fact that led to plotting the curves of figure 10 in reference 3. Thus, for instance, for $r = 16$ inches and $S = 10$, n is about 2.75; while for $r = 16$ inches and for $S = 40$, n is found to be about 5.

Determination of the Value of n

The value of n can be calculated from equation (26) of reference 3. Substituting n for p and solving for n yields

$$n^2 = \left[\gamma^2 + \frac{I_{str\ s}\ \Lambda_s}{\lambda_s^4\ I_{str\ r}}\right]^{1/2} - \gamma \qquad (41)$$

$$\gamma = (5/16)(I_{str\ t}/I_{str\ r}) \qquad (41a)$$

To facilitate the calculation of n, graphs of γ

and $I_{str\ s}/I_{str\ r}$ were drawn against ϵ_{max}, the data being taken from the foregoing graphs. The γ curves are presented in figure 13a, the $I_{str\ s}/I_{str\ r}$ curves in figure 13b. With the aid of these figures n can be easily calculated from equation (41).

It may be mentioned that a transformation of equation (41) permits a further simplification in the calculations. The second term on the right-hand side can be written in the form

$$\frac{I_{str\ s}\,\Lambda_s}{\lambda_s^4\,I_{str\ r}} = \frac{I_{str\ s}(r^4/L_1^3 d)(I_{str\ s}/I_{str\ r})}{(\pi/L_1)^4[I_{str\ s}/(A + 2wt)\,\epsilon_{max}]^2 I_{str\ r}}$$

By use of the identity

$$S = 2\pi r/d$$

there is obtained

$$I_{str\ s}\Lambda_s\,/(\lambda_s^4 I_{str\ r})$$

$$= SL_1 r^3[\epsilon_{max}(A + 2wt)]^2/[2\pi^5 I_r I_{str\ r}] = \xi\,\epsilon_{max}^2 \qquad (42)$$

In figure 14 $\xi\,\epsilon_{max}^2/L_1$ is plotted against ϵ_{max} for r = 10 inches. The two curves shown correspond to S = 12 and S = 24.

Substituting back into equation (41) results in the following expression for n^2:

$$n^2 = (\gamma^2 + \xi\,\epsilon_{max}^2)^{1/2} - \gamma \qquad (43)$$

Equation (43) is identical with the solution of the quadratic in n^2 that is obtained from equation (20) of reference 3 if the value of I_{str} is substituted and the equation divided by (A + 2wt)E. By using figures 13a and 14, the values of n can be calculated rapidly from equation (43).

Figure 15 contains values of n plotted against

ϵ_{max} for the 63 specimens investigated in this report. The diagram shows that with each type of specimen in tests involving different ratios of bending moment and shear all test points obtained lie on a curve resembling a parabola.

Number of Rings Involved

The number m of rings involved in a wave at buckling can be calculated from equations (14), (16), and (18) of reference 3:

$$m = 2.84 \lambda_n - 1 \tag{44}$$

In this equation λ_n is the correct value of the equivalent length factor. Since λ_3 and n were calculated previously for all the specimens, a simple way of obtaining λ_n is by the use of the formula

$$\lambda_n = \lambda_3 [(2/n)(5/16)(I_{str\ t}/I_{str\ 3}) + (I_{str\ r}/I_{str\ 3})]^{1/2} \tag{45}$$

The value of λ_n should be an integer less than or equal to the total number of rings in the monocoque cylinder. If the value calculated from the formula is not an integer, the closest integer should be used. Table I contains the number m as calculated from equations (44) and (45) with the aid of the graphs previously discussed. It should be mentioned that cumulative errors in the numerical calculations easily may have the effect of shifting the closest integer value by 1. Nevertheless the table shows that the number m of rings required by theory was available in every one of the specimens.

Variation of n with 2w

In figure 16 values of n are plotted against $\epsilon^2_{max}\ SL_1$ for r = 10 inches and different values of 2w. The curves were calculated from equation (43). They were replotted in figure 17 as n against 2w curves. For low values of the parameter $\epsilon^2_{max}\ SL_1$ (corresponding to

low values of n) these curves are nearly horizontal from $2w = 0$ to $2w = 1$; then they drop off considerably. However, as the parameter increases, the curves slope up to a flat maximum and then decline less rapidly than the curves just discussed. In general, over the working range n changes only about 5 percent, barring the drop at low values of the parameter.

Hence it is logical to choose $2w$ = constant for all the specimens, for instance, $2w = 1$ inch, or possibly $2w = 0$. If this is done, equation (43) reduces to a simpler form which when solved for ϵ_{max} yields the expression

$$\epsilon_{max} = n[(n^2 - 2\gamma)/\xi]^{1/2} \qquad (46)$$

in which the symbols γ and ξ have values defined by equations (41a) and (42), respectively. These parameters may be calculated with the aid of any convenient assumption for $2w$.

The Effect of the Shearing Force

In order to show how the shear force affects the value of the parameter n, the calculated values were superimposed upon the line diagram of figure 10 of reference 3 which represents the variation of n with two characteristic parameters in the case of pure bending. It may be seen from figure 18 (or from table II) that the agreement is reasonably good. If the four specimens that failed according to the shear pattern and the one that failed in panel instability are disregarded, analysis of the test results gives the following data: 22 specimens deviated from the curves less than 5 percent; 17, between 5 and 10 percent; 9, between 10 and 15 percent; 7, between 15 and 20 percent; 1, 21 percent; and 1, 41 percent. This variation is more evident in figure 19 where the calculated n's are plotted against the predicted n's.

It may be seen from table II that the applied moment is approximately proportional to the number of stringers in the specimen, everything else being equal. This shows that the sheet carries comparatively little load.

One of the main objects of the present investigation was to determine the effect of the shear force upon the

buckling load in general instability. The first group in table II consists of four specimens having 10 stringers and a ring spacing of 2 inches. In this group the bending moment at buckling decreases from 105,500 to 72,100 inch-pounds as the arm decreases from 128 to 66.5 inches. In the group containing the four specimens 122 to 125 having 12 stringers and a ring spacing of 2 inches, the tendency is reversed. The bending moment at buckling increases from 188,000 to 214,000 inch-pounds, while the moment arm decreases from 113 to 40.5 inches. Consideration of all the data reveals that both these tendencies are found in several of the groups; while in others irregular oscillations or practically constant values prevail. Similar observations can be made concerning the variation of ϵ_{max}, although the changes in these values are much smaller. Consequently the only statement that can be made on the basis of the present experiments is that the variation of the critical strain in general instability is little but unpredictably influenced by the presence of a shear force.

THE BUCKLING INEQUALITY

The airplane designer is interested in determining quickly whether the fuselage he has designed is likely to fail in general instability. In the following an inequality is developed which can be used for this purpose.

Substitution of equation (38) into equation (37) gives

$$P_{cr\ gi} = \pi^2 E_{str} I_{str} / [L_1 (\sqrt[4]{\Lambda/n})]^2 \qquad (47)$$

where the letters gi indicate that failure occurs in general instability. If the letter p is used to indicate panel instability, the following equation may be written:

$$P_{cr\ p} = \pi^2 E_{str} I_{str\ r} / (L_1 \lambda_p)^2 \qquad (48)$$

where λ_p is the effective length factor in panel instability. Its value must lie between 1 and 1/2; with stringers continuous through the rings it may be taken as

$1/\sqrt{2}$. Obviously general instability will not occur if

$$P_{cr\ gi} > P_{cr\ p} \tag{49}$$

Substitution of equations (47) and (48) into equation (49) gives, after some transformations,

$$\Lambda < (I_{str}/I_{str\ r})^2 n^4 \lambda_p^4 \tag{50}$$

If inequality (50) is satisfied, general instability will not occur. Unfortunately, however, the values of the symbols appearing in the inequality are not too easily computed, since the calculations involve the assumption of n, and the subsequent determination of the moments of inertia and of Λ with the aid of this assumed value. A simpler, though approximate, inequality may be obtained in the following manner: After substitution of Λ from equation (17), inequality (50) can be transformed to read:

$$[r^4/(L_1^3 d)](I_{str\ r}^2/I_r I_{str})(E_{str}/E_r) < n^4 \lambda_p^4 \tag{a}$$

Since by definition $I_{str\ r}/I_{str}$ is less than unity, general instability is certainly impossible if

$$[r^4/L_1^3 d)](I_{str\ r}/I_r)(E_{str}/E_r) < n^4 \lambda_p^4 \tag{b}$$

It follows from experimental evidence that n is very unlikely to be less than 2.5. If n is assumed to be 2.5, and λ_p to be $1/\sqrt{2}$, the right-hand side of inequality (b) becomes approximately 10. Consequently the condition under which general instability cannot occur is the inequality

$$[r^4/(L_1^3 d)](E_{str} I_{str\ r}/E_r I_r) < 10 \tag{51}$$

In this inequality $I_{str\ r}$ should be calculated on the assumption of a reasonable value for the effective width $2w_{curved}$. In most cases correct results should be obtained even if the effective width is disregarded, since all the assumptions made in the development caused deviations to the safe side. When the moment of inertia of the stringer

in the radial direction is computed without the effective width of sheet and the moment of inertia of the ring likewise, the left-hand side of inequality (51) may be called the reduced buckling index. With the so-calculated moment of inertia denoted $I_{str\ o}$, and the reduced buckling index Λ_o, inequality (51) may be written in the concise form

$$\Lambda_o < 10 \tag{52}$$

where

$$\Lambda_o = [r^4/(L_1^3 d)](E_{str} I_{str\ o}/E_r I_{r\ o}) \tag{52a}$$

Inequality (52) is the condition under which general instability cannot occur. It may be used conveniently for the determination of the required size of the ring section when the other structural data of the monocoque cylinder are given.

It is possible that experience with actual monocoque fuselages will permit raising the value of the right-hand side of inequality (52), perhaps to as high as 30.

COMPARISON OF PREDICTED AND EXPERIMENTAL CRITICAL STRAIN

In table III the experimental critical strain is compared with the critical strain calculated according to the procedure developed in this report and in reference 3. In this procedure the value of n is taken from the curves of figure 18 of this report (or figure 10 of reference 3) corresponding to an assumed value of the critical strain ϵ_{max} and the dimensions of the monocoque cylinder. Then $P_{cr\ tot}$ is calculated from equation (24) of this report. It should be noted that the effective width of sheet must be considered in the calculation of the moments of inertia, and that the value of ν is zero for all the cylinders listed in table III. The strain obtained by dividing $P_{cr\ tot}$ by the cross-sectional area of stringer plus effective sheet and by Young's modulus is compared with the assumed value of

ϵ_{max}. The procedure is repeated with a modified assumption of the value of the critical strain until assumed and calculated values agree closely enough for practical purposes.

In the present case the actual calculations were carried out with the aid of figure 15 of this report which represents a theoretical relationship between n and ϵ_{max}. The procedure then reduced to finding the value of ϵ_{max} that was connected with the same value of n both in figures 15 and 18.

The accuracy of the predictions may be judged from figure 20 in which the calculated critical strain is plotted against the experimental critical strain. In judging the figure it should not be forgotten that the theory does not take into account the effect of the shear force.

AVAILABLE EXPERIMENTAL EVIDENCE OF THE VALIDITY OF THE BUCKLING INEQUALITY

In table IV the value of the reduced buckling index Λ_0 is listed for cylinders Nos. 25 to 129 of the GALCIT investigations reported in references 2 and 4. In addition, values computed for five actual airplane fuselages are given.

It may be seen that every specimen having a reduced buckling index greater than 181 failed in general instability (unless failure was due to tension or shear). Moreover, every specimen having a reduced buckling index smaller than 37.7 failed in panel instability. There were too few specimens in the region between $\Lambda_0 = 10$ and $\Lambda_0 = 200$ to permit a final conclusion to be drawn concerning the value of Λ_0 below which general instability cannot occur.

It may be noted that four of the five actual airplane fuselages listed have Λ_0 values well below 10 so that for these four general instability is impossible. For Lockheed Model 27, however, $\Lambda_0 = 71.38$. This

airplane fuselage, therefore, may fail either in general or panel instability.

CONCLUSIONS

1. The total load carried by the most highly compressed stringer, together with its effective width of sheet, in a circular monocoque cylinder loaded simultaneously in bending and compression, can be written in the form

$$P_{cr\ tot} = n^2 \sqrt{\frac{d}{L_1} \frac{\pi^2 \sqrt{E_{str} I_{str} E_r I_r}}{r^2}} - \frac{0.9}{n^2} \nu\, d \qquad (24)$$

It follows from equation (24), and from the experimental evidence according to which n is seldom less than 3, that the total buckling load $P_{cr\ tot}$ is little influenced by the ratio of bending moment to compressive load as long as the compressive load is so small that it does not change the inward bulge pattern. This conclusion is valid only if n is not influenced by the compressive force. Whether this is the case will be investigated experimentally and the results will be presented in part II of this report.

2. If the direct stress distribution in a bent circular monocoque cylinder deviates from the linear law, the maximum effect upon the critical stress in the inward bulge type buckling is a reduction in the ratio 1 to $[1 + (0.9/n^2)]$. Since n is seldom less than 3, the reduction is slight. This conclusion holds only if the change in the stress distribution does not cause a change in the value of n. If the contrary is true, the effect may be greater, and the critical load must then be calculated from equation (27).

3. Investigation of the 55 reinforced monocoque cylinders tested at GALCIT in combined bending and shear shows reasonable agreement with the theory of reference 3. The variation of the critical strain with shear force is slight and inconsistent.

4. A simple approximate formula is suggested for the use of the designer to predict the likelihood of the occurrence of general instability, and for the determination of the moment of inertia of the rings required for excluding the possibility of general instability. The formula is written as an inequality

$$\Lambda_o < 10 \tag{52}$$

where the reduced buckling index

$$\Lambda_o = [r^4/(L_{id}^3)](E_{str}I_{str\ o}/E_rI_{r\ o}) \tag{52a}$$

In equation (52a) each symbol represents a simple geometric or mechanical property of the structure, so that the reduced buckling index can be easily calculated. If its value satisfies inequality (52) - that is, if it is less than 10 - general instability does not occur. It is possible that experience with actual monocoque fuselages will permit raising the value of the right-hand side of inequality (52), perhaps to as high as 30.

Polytechnic Institute of Brooklyn,
Brooklyn, N. Y., January 1944.

REFERENCES

1. Hoff, N. J.: Instability of Monocoque Structures in Pure Bending. Jour. R.A.S., vol. XLII, no. 328, April 1938, pp. 291-346.

2. Guggenheim Aeronautical Laboratory, California Institute of Technology: Some Investigations of the General Instability of Stiffened Metal Cylinders.
I - Review of Theory and Bibliography. NACA TN No. 905, 1943.
II - Preliminary Tests of Wire-Braced Specimens and Theoretical Studies. NACA TN No. 906, 1943.
III - Continuation of Tests of Wire-Braced Specimens and Preliminary Tests of Sheet-Covered Specimens. NACA TN No. 907, 1943.
IV - Continuation of Tests of Sheet-Covered Specimens and Studies of the Buckling Phenomena of Unstiffened Circular Cylinders. NACA TN No. 908, 1943.
V - Stiffened Metal Cylinders Subjected to Pure Bending. NACA TN No. 909, 1943.

3. Hoff, N. J.: General Instability of Monocoque Cylinders. Jour. Aero. Sci., vol. 10, no. 4, April 1943, pp. 105-114.

4. Guggenheim Aeronautical Laboratory, California Institute of Technology: Some Investigations of the General Instability of Stiffened Metal Cylinders.
VI - Stiffened Metal Cylinders Subjected to Combined Bending and Transverse Shear. NACA TN No. 910, 1943.

TABLE I

Spec. No.	(1) $\frac{5}{16}\frac{I_{str.t}}{I_{str.r}}$	(2) $\frac{I_{str.3}}{I_{str.r}}$	(3) n^2	(4) λ_3	(5) 2(1)/(3)(2)	(6) (5)+1/(2)	(7) $m=(2.84)[(4)\sqrt{(6)}]-1$	(8) * +
			Number of Rings Involved in Failure					
84	3.41	1.762	7.71	5.13	.502	1.070	14.05	31
85	3.93	1.864	6.77	5.44	.623	1.160	15.63	31
86	3.29	1.734	8.01	5.02	.474	1.050	13.60	31
87	3.39	1.755	7.81	5.10	.494	1.064	13.96	31
83	5.83	2.293	7.37	3.31	.690	1.126	8.96	15
118	1.052	1.233	7.79	3.36	.2195	1.020	8.61	19
119	1.048	1.230	7.89	3.33	.216	1.029	8.59	19
120	1.062	1.238	7.67	3.39	.224	1.032	8.76	19
121	1.009	1.233	8.17	3.22	.202	1.013	8.19	19
111	1.546	1.358	7.55	2.09	.302	1.039	5.05	9
112	1.310	1.300	8.48	1.91	.238	1.007	4.62	9
113	1.430	1.333	8.01	2.06	.268	1.018	4.91	9
109	2.41	1.540	7.74	1.28	.404	1.053	2.72	4
110	1.97	1.374	10.50	1.07	.273	1.001	2.04	4
79	1.01	1.227	16.2	3.88	.1021	0.918	9.58	31
80	1.276	1.286	12.23	4.52	.1622	0.940	11.48	31
81	1.125	1.250	14.12	4.17	.1279	0.927	10.40	31
82	1.426	1.324	10.91	4.82	.1975	0.952	12.38	31
88	1.248	1.279	18.21	2.23	.1071	0.890	4.98	15
89	1.424	1.325	15.83	2.41	.1360	0.891	5.45	15
90	1.282	1.290	17.71	2.27	.1122	0.887	5.07	15
91	1.380	1.312	16.57	2.36	.1270	0.890	5.34	15
126	1.294	1.292	17.56	2.28	.1141	0.888	5.11	15
127	1.40	1.319	16.26	2.39	.1310	0.890	5.44	15
128	1.288	1.290	17.61	2.27	.1135	0.889	5.08	15
129	1.307	1.296	17.42	2.29	.1100	0.889	5.13	15

TABLE I cont'd.

Spec. No.	(1) $\frac{5}{16}\frac{I_{str.t}}{I_{str.r}}$	(2) $\frac{I_{str.3}}{I_{str.r}}$	(3) n^2	(4) λ_3	(5) 2(1)/(3)(2)	(6) (5)+1/(2)	(7) $m=(2.84)[(4)\sqrt{(6)}]-1$	(8) * +
			Number of Rings Involved in Failure					
75	1.76	1.385	20.73	1.33	.1230	0.895	2.58	7
76	1.88	1.42	18.43	1.384	.1439	0.848	2.62	7
77	1.915	1.425	18.28	1.387	.1474	0.849	2.64	7
78	1.92	1.43	18.26	1.390	.1473	0.847	2.64	7
92	1.902	1.423	18.29	1.390	.1464	0.849	2.64	7
93	2.25	1.494	16.20	1.495	.1859	0.856	2.94	7
122	.50	1.100	11.43	5.29	.0796	0.989	13.95	39
123	.51	1.101	10.77	5.46	.0862	0.995	14.50	39
124	.51	1.104	10.49	5.53	.0880	0.994	14.68	39
125	.51	1.105	10.49	5.53	.0880	0.993	14.68	39
69	.54	1.116	13.37	2.95	.0726	0.970	7.26	19
70	.53	1.110	13.83	2.89	.0691	0.970	7.09	25
71	.51	1.103	15.44	2.73	.0600	0.967	6.64	15
72	.495	1.100	16.84	2.61	.0535	0.969	6.28	11
106	.558	1.12	12.88	2.94	.0775	0.970	7.24	19
107	.526	1.11	14.79	2.86	.0641	0.965	7.00	19
108	.557	1.12	12.98	2.93	.0767	0.970	7.21	19
65	.63	1.135	14.28	1.72	.0779	0.960	3.80	12
66	.63	1.135	14.28	1.72	.0779	0.960	3.80	9
67	.604	1.30	15.30	1.66	.0607	0.830	3.30	7
68	.59	1.128	16.41	1.60	.0638	0.951	3.44	5
98	.602	1.130	15.50	1.65	.0688	0.954	3.59	5
99	.613	1.140	14.99	1.68	.0717	0.950	3.66	5
100*	.688	1.152	12.21	1.87	.0978	0.967	4.23	5
101*	.672	1.149	12.58	1.84	.0932	0.963	4.13	5

TABLE I cont'd.

Number of Rings Involved in Failure

Spec. No.	(1) $\frac{5}{16}\frac{I_{str.t}}{I_{str.r}}$	(2) $\frac{I_{str.i}}{I_{str.r}}$	(3) n^2	(4) λ_3	(5) 2(1)/(3)(2)	(6) (5)+1/(2)	(7) $m=(2.84)[(4)/(6)]-1$	(8) * +
94+	1.00	1.223	11.08	1.20	.1479	0.966	2.35	4
95	.66	1.144	19.15	0.882	.0603	0.934	1.42	4
96	.696	1.153	16.70	0.946	.0723	0.948	1.64	4
97*	.85	1.190	13.23	1.09	.1079	0.949	2.02	4
102	.58	1.128	23.51	3.66	.0438	0.932	9.00	31
103	.59	1.130	23.26	3.68	.0449	0.930	9.01	31
104	.54	1.119	29.38	3.29	.0329	0.937	8.05	31
105*	.67	1.150	17.56	4.22	.0664	0.936	10.60	31
114	.67	1.151	25.35	2.11	.0459	0.917	4.74	15
115	.72	1.160	23.54	2.23	.0528	0.916	5.07	15
116	.67	1.150	25.85	2.10	.0451	0.915	4.73	15
117*	.945	1.210	16.10	2.71	.0971	0.923	6.41	15

(1) taken from figure 13.a

(2) taken from figure 13.b

(3) calculated from Eq. 41

(4) taken from figure 11

(8) * total number of rings in the structure

+ Failure is general instability unless indicated by

* shear

\+ panel

TABLE II

Summary of Data

Spec. No.	s	l_1 inches	** $\epsilon_{max.} \times 10^6$	shear load lbs.	sra to fixed end inches	maximum moment in.-lb.	$\times 10^{-3}$ n	Δn**
84			212	825	128	105.5	2.78	1.1
85			195	915	104	95.2	2.60	-5.5
86	10	2	218	915	80	73.2	2.83	2.9
87			213	929	66.5	61.8	2.79	1.4
83		4	154	563	128	72.1	2.72	-2.5
118			360	710	113	80.2	2.79	-5.7
119			364	990	88.4	87.4	2.81	-4.4
120		2	353	1460	65	95.0	2.77	-6.0
121			376	2310	40.5	93.6	2.86	-2.4
111	12		251	660	113	74.6	2.75	-8.9
112		4	290	1780	40.5	72.2	2.95	-1.6
113			265	930	88.4	82.3	2.83	-6.6
109			186	450	113	50.8	2.78	-9.7
110		6	242	1470	40.5	59.6	3.24	6.6
79			290	2000	128	256	4.02	19.0
80			211	1850	107	198	3.45	-4.2
81		2	242	2175	86	187	3.76	8.0
82			189	2070	64	133	3.30	-9.6
88			216	2115	80	169	4.27	18.5
89			187	1910	66.5	192	3.98	7.6
90			209	1312	128	168	4.21	17.0
91			194	1331	116	155	4.07	11.0
126	20	4	207	1600	109	175	4.19	16.5
127			192	1940	89	173	4.03	10.0
128			206	1445	137	198	4.20	16.5
129			205	2340	65	152	4.17	12.5

TABLE II cont'd.

Summary of Data

Spec. No.	S	L_1 inches	++ $\epsilon_{max.} \times 10^6$	shear load lbs.	arm to fixed end inches	maximum moment in.-lb. $\times 10^{-3}$	n	Δn++
75			161	1057	128	135	4.54	21.0
76			150	1050	116	122	4.29	12.5
77		8	1516	1450	92	134	4.28	12.5
78			151	995	116	115	4.28	12.5
92			152	503	194	97.6	4.28	12.5
93			135	1353	74	100	4.03	4.6
122			525	1665	113	188	3.38	0.0
123	24	1	492	2140	88.4	189	3.28	-3.7
124			481	3220	65	210	3.24	-6.0
125			479	5280	40.5	214	3.24	-6.0
69			420			L/D 2.0	3.66	0.0
70			440	Pure Bending		2.6	3.72	2.7
71	24	2	490			1.6	3.93	14.0
72			540			1.2	4.10	11.5
106			396	1490	113	168	3.60	-2.5
107			450	2760	65	179	3.76	5.5
108			398	4270	40.5	173	3.61	-2.5
65			315			L/D 2.6	3.77	-2.6
66			315	Pure Bending		2.0	3.77	-2.6
67			398			1.6	3.91	2.6
68			355			1.2	4.05	6.5
98	24	4	340	1310	113	148	3.94	2.0
99			330	1660	88.4	147	3.87	1.5
100*			270	2250	65	147	3.49	—
101*			280	3370	40.5	134	3.55	—

TABLE II cont'd.

Summary of Data

Spec. No.	S	L_1 inches	++ $\epsilon_{max.} \times 10^6$	shear load lbs.	arm to fixed end inches	maximum moment in.-lb. $\times 10^{-3}$	n	Δn++
94+			174	960	114	110	3.33	—
95		8	290	1283	88.4	113	4.38	12.0
96			265	1711	65	111	4.09	2.2
97*			207	2900	40.5	118	3.64	—
102			282	2480	137	340	4.85	18.8
103			277	2840	112.4	321	4.82	18.0
104		2	343	4200	89	374	5.36	41.0
105*	40		218	4500	65.1	293	4.19	—
114			216	1900	137	261	5.04	5.5
115			194	2010	112.4	226	4.85	-3.0
116		4	217	2400	89	216	5.06	5.5
117*			136	2450	65.3	160	4.01	—

Footnotes:

++ ϵ_{Max} is the strain reading taken with a 16 in. wire gage which extended from 6 to 22 in. from the fixed end of the structure.

+++ Δn is the percentage departure of the calculated values of n from the pure bending curves of reference 3.

Failure is general instability unless indicated by

* Shear

\+ Panel

Table III. Comparison of Calculated and Observed Critical Strain.

GALCIT Spec.No.	Calculated $\epsilon_{max} \times 10^6$	Observed $\epsilon_{max} \times 10^6$	GALCIT Spec. No.	Calculated $\epsilon_{max} \times 10^6$	Observed $\epsilon_{max} \times 10^6$
84	205	212	122	525	525
85	205	195	123	525	492
86	205	218	124	525	481
87	205	213	125	525	479
83	158	154	69	420	420
118	383	360	70	420	440
119	383	364	71	420	490
120	383	353	72	420	540
121	383	374	106	420	396
111	292	251	107	420	450
112	292	290	108	420	398
113	292	265	65	325	315
109	220	186	66	325	315
110	220	242	67	325	338
79	215	290	68	325	355
80	215	211	98	325	340
81	215	242	99	325	330
82	215	189	95	290	290
88	170	216	96	250	265
89	170	187	102	230	282
90	170	209	103	230	277
91	170	194	104	230	343
126	170	207	114	200	216
127	170	192	115	200	194
128	170	208	116	200	217
129	170	205			
75	125	161			
76	125	150			
77	125	1516			
78	125	151			
92	125	152			
93	125	135			

Table IV. Reduced Buckling Index.

$$\Lambda_o = (r^4/L_1^3 d)(I_{str\ o}/I_{ro})$$

GALCIT Spec. No.	r	L_1	d	$(r^4/L_1^3 d)$	Λ_o	Type of failure*
25	15.92	8	2.53	49.59	1207	G
26	15.92	4	2.53	396.7	9652	G
27	15.92	2	2.53	3174	77220	G
28	15.92	16	2.53	6.199	150.8	P/G
29	15.92	16	5.06	3.099	75.41	P
30	15.92	8	5.06	24.80	603.3	G
31	15.92	4	5.06	198.4	4827	G
32	15.92	2	5.06	1587	38610	G
34	15.92	16	10.12	1.550	37.70	P/G
35	15.92	8	10.12	12.40	301.6	G
36	15.92	4	10.12	99.18	2413	G
37	15.92	2	10.12	793.5	19310	G
38	15.92	1	10.12	6347	154000	G
39	15.92	1	2.53	25390	617800	G
40	15.92	16	2.53	6.199	150.8	P
41	15.92	8	2.53	49.59	1207	G
42	15.92	4	2.53	396.7	9652	G
43	15.92	2	2.53	3174	77220	G
44	15.92	16	5.06	3.099	75.41	P
45	15.92	8	5.06	24.80	603.3	G
46	15.92	4	5.06	198.4	4827	G
47	15.92	2	5.06	1587	38610	G
48	15.92	16	10.12	1.550	37.70	P
49	15.92	8	10.12	12.40	301.6	G
50	15.92	4	10.12	99.18	2413	G
51	15.92	2	10.12	793.5	19310	G
52	16	16	2.53	6.324	7.581	P
53	16	8	2.53	50.59	60.65	P
54	16	4	2.53	404.7	485.2	G
55	16	2	2.53	3238	3882	G
56	16	16	5.06	3.162	3.791	P
57	16	8	5.06	25.30	30.33	P
58	16	4	5.06	202.3	242.5	G
59	16	2	5.06	1619	1941	G
60	16	8	5.06	25.30	34.53	P
61	16	4	5.06	202.3	276.1	G
62	16	2	5.06	1619	2209	T
63	16	4	2.53	404.7	552.4	G
64	16	2	2.53	3238	4420	G
65	10	4	2.61	59.87	1457	G
66	10	2	2.61	478.9	11650	G
67	10	4	5.22	29.94	728.4	G
68	10	2	5.22	239.4	5825	G
69	10	4	2.61	59.87	1457	G
70	10	2	2.61	478.9	11650	G
71	10	4	5.22	29.94	728.4	G
72	10	2	5.22	239.4	5825	G
73	10	4	2.61	59.87	1457	G
74	10	2	2.61	478.9	11650	G
75	16	8	5.06	25.30	615	G
76	16	8	5.06	25.30	615	G
77	16	8	5.06	25.30	615	G

* G means general, P panel instability, P/G start by panel and final failure by general instability. T indicates tension failure, J shear failure

Table IV (continued)

	GALCIT Spec. No.	r	L_1	d	$(r^4/L_1^3 d)$	Λ_o	Type of failure*
	78	16	8	5.06	25.30	615	G
	79	16	2	5.06	1619	39350	G
	80	16	2	5.06	1619	39350	G
	81	16	2	5.06	1619	39350	G
	82	16	2	5.06	1619	39350	G
	83	16	4	10.12	101.2	39350	G
	84	16	2	10.12	809.5	39350	G
	85	16	2	10.12	809.5	39350	G
	86	16	2	10.12	809.5	39350	G
	87	16	2	10.12	809.5	39350	G
	88	16	4	5.06	202.4	4925	G
	89	16	4	5.06	202.4	4925	G
	90	16	4	5.06	202.4	4925	G
	91	16	4	5.06	202.4	4925	G
	92	16	8	5.06	25.3	615	G
	93	16	8	5.06	25.3	615	G
	94	10	8	2.62	7.454	181	P
	95	10	8	2.62	7.454	181	G
	96	10	8	2.62	7.454	181	G
	97	10	8	2.62	7.454	181	S
	98	10	4	2.62	59.64	1450	G
	99	10	4	2.62	59.64	1450	G
	100	10	4	2.62	59.64	1450	S
	101	10	4	2.62	59.64	1450	S
	102	16	2	2.53	3238	76350	G
	103	16	2	2.53	3238	76350	G
	104	16	2	2.53	3238	76350	G
	105	16	2	2.53	3238	76350	S
	106	10	2	2.62	477.1	11600	G
	107	10	2	2.62	477.1	11600	G
	108	10	8	2.62	7.454	181	G
	109	10	8	5.24	3.727	90.6	G
	110	10	8	5.24	3.727	90.6	G
	111	10	4	5.24	29.82	725	G
	112	10	4	5.24	29.82	725	G
	113	10	4	5.24	29.82	725	G
	114	16	4	2.53	404.7	9840	G
	115	16	4	2.53	404.7	9840	G
	116	16	4	2.53	404.7	9840	G
	117	16	4	2.53	404.7	9840	S
	118	10	2	5.24	238.5	5800	G
	119	10	2	5.24	238.5	5800	G
	120	10	2	5.24	238.5	5800	G
	121	10	2	5.24	238.5	5800	G
	122	10	1	2.62	3817	92800	G
	123	10	1	2.62	3817	92800	G
	124	10	1	2.62	3817	92800	G
	125	10	1	2.62	3817	92800	G
	126	16	4	5.06	202.4	4925	G
	127	16	4	5.06	202.4	4925	G
	128	16	4	5.06	202.4	4925	G
	129	16	4	5.06	202.4	4925	G
Lockheed Model	10	27	30	8	2.464	0.1308	-
" "	12	30	24	6	9.766	0.5762	-
" "	14	35	24	8	13.63	0.9091	-
" "	27	63	16	4	963.3	71.38	-
Douglas "	DC-4	66	24	5.5	249.6	3.844	-

* G means general, P panel instability, P/G start by panel and final failure by general instability. T indicates tension failure, S shear failure.

FIG. 1

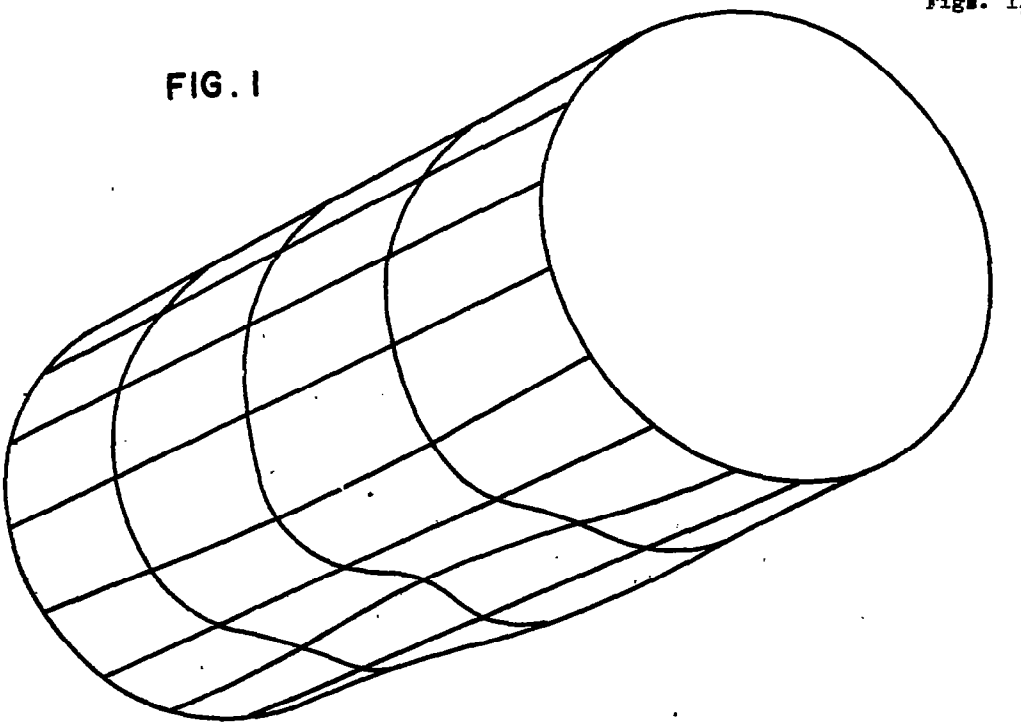

FIG. 2

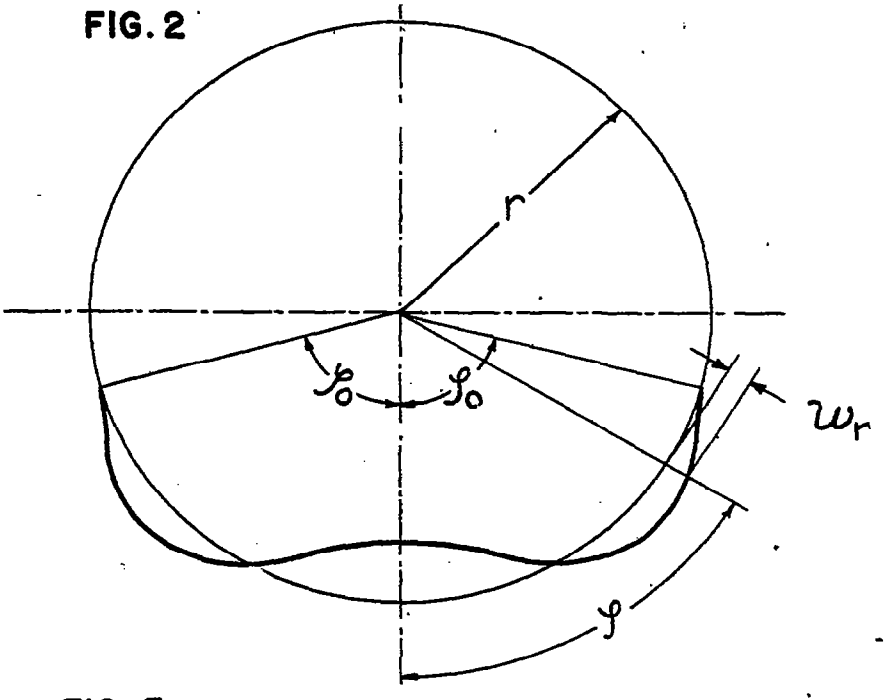

FIG. 3

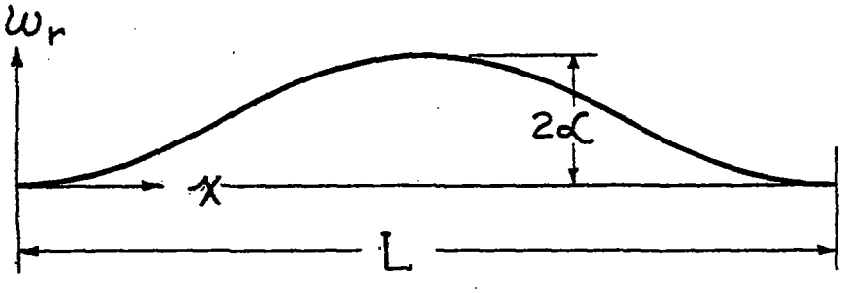

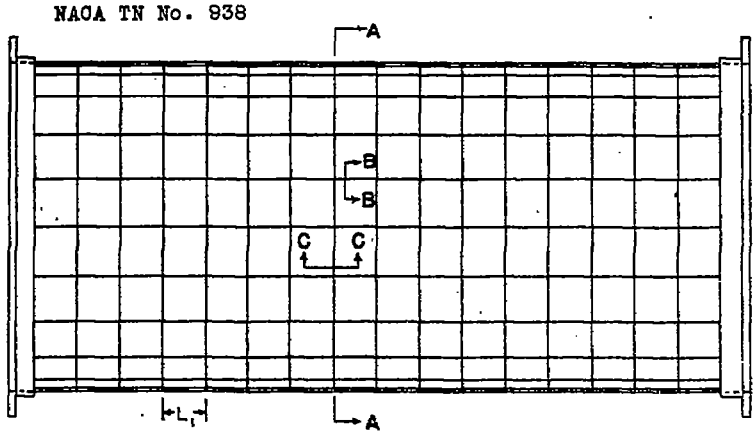

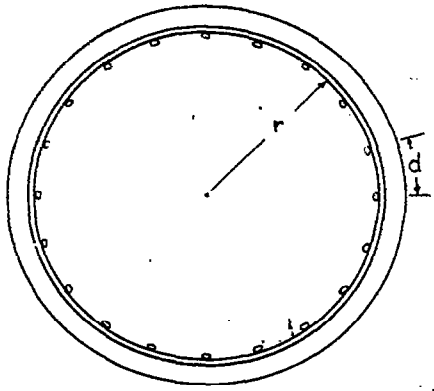

SECTION A-A

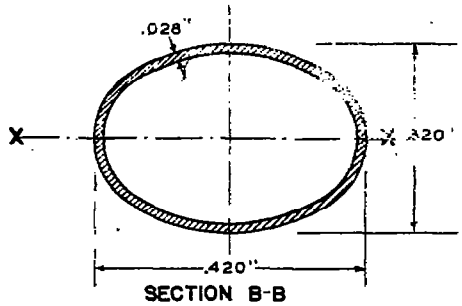

SECTION B-B

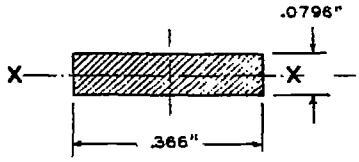

SECTION C-C

FIG. 4. SCHEMATIC DRAWING OF MONOCOQUE CYLINDER
THICKNESS OF SHEET t = .010 IN.

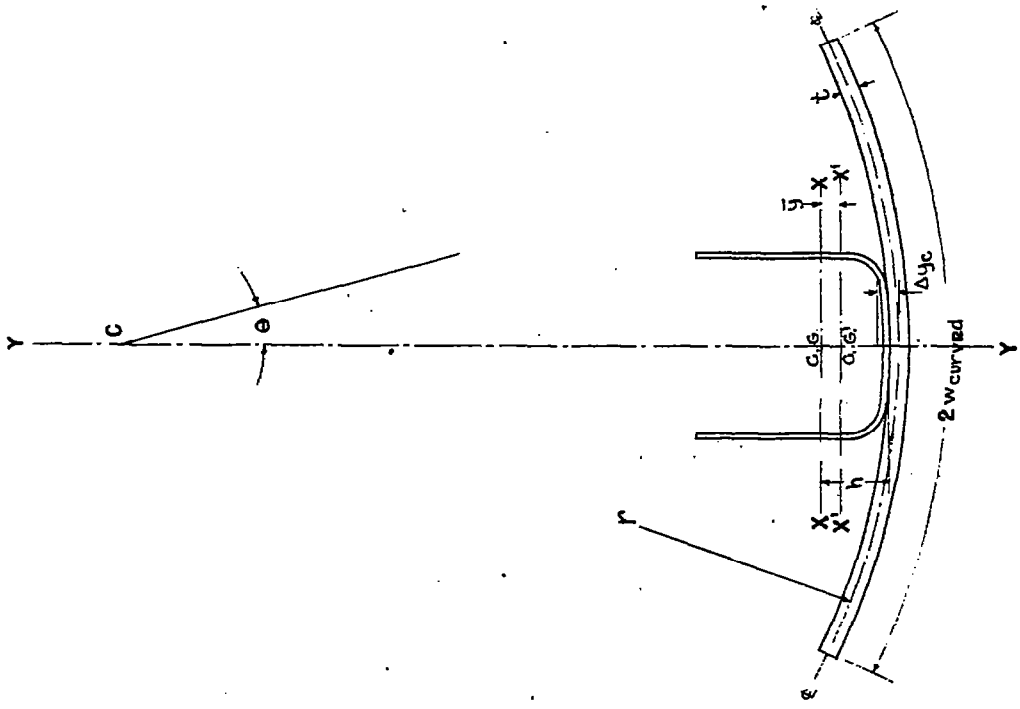

FIG. 6. CURVED SHEET AND STRINGER.

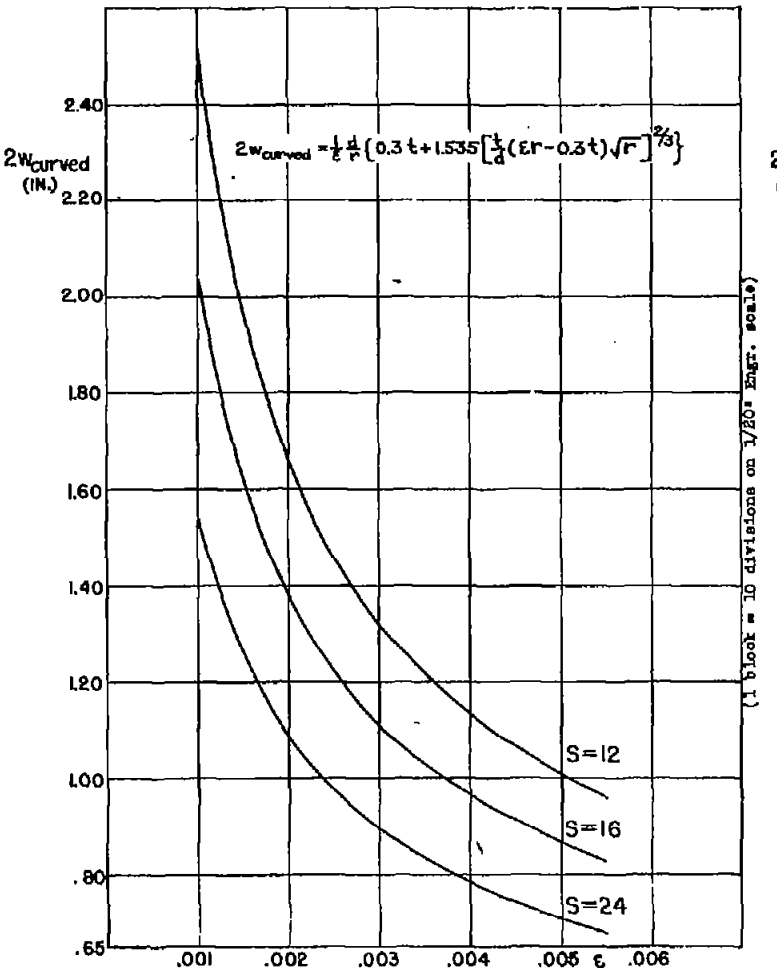

FIG. 5a. $2w_{curved}$ VS. ε
FOR r = 10 IN.

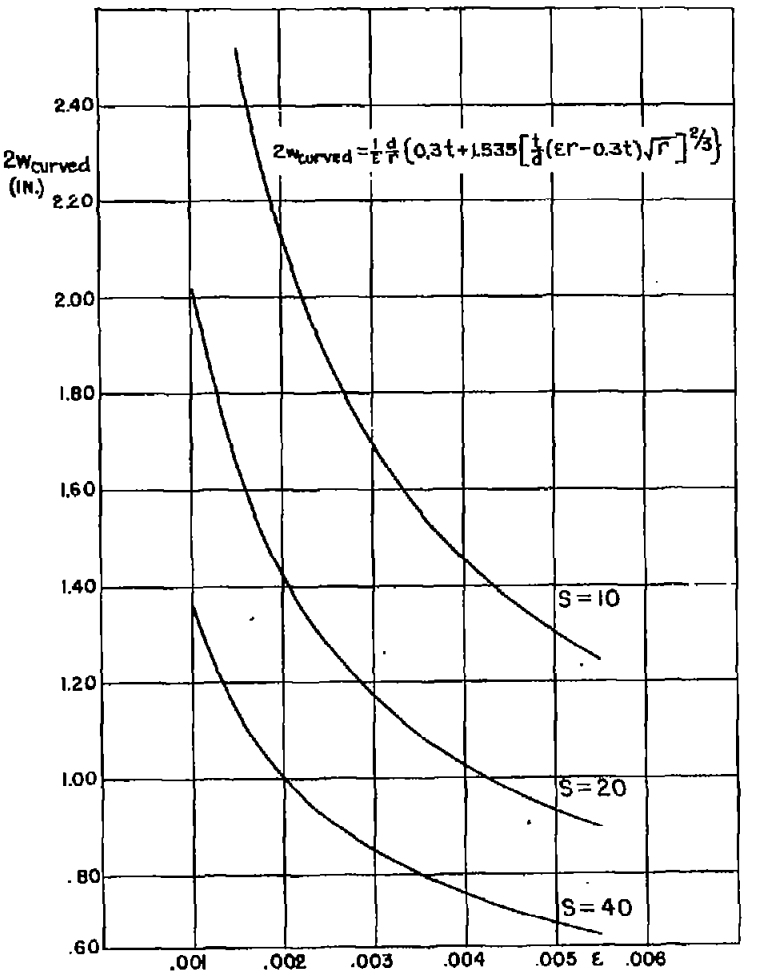

FIG. 5 b. $2w_{curved}$ VS. ε
FOR r = 16 IN.

Fig. 5

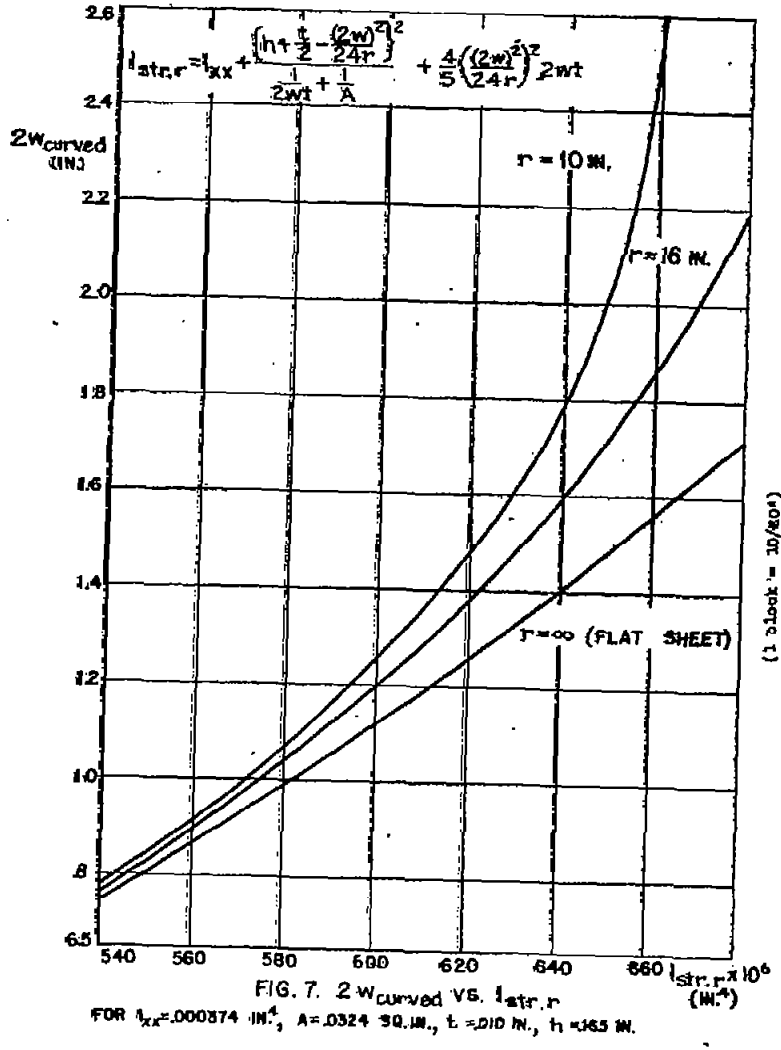

FIG. 7. $2w_{curved}$ vs. $I_{str.r}$
FOR I_{xx}=.000874 IN.^{4}, A=.0324 SQ.IN., t =.010 IN., h =.165 IN.

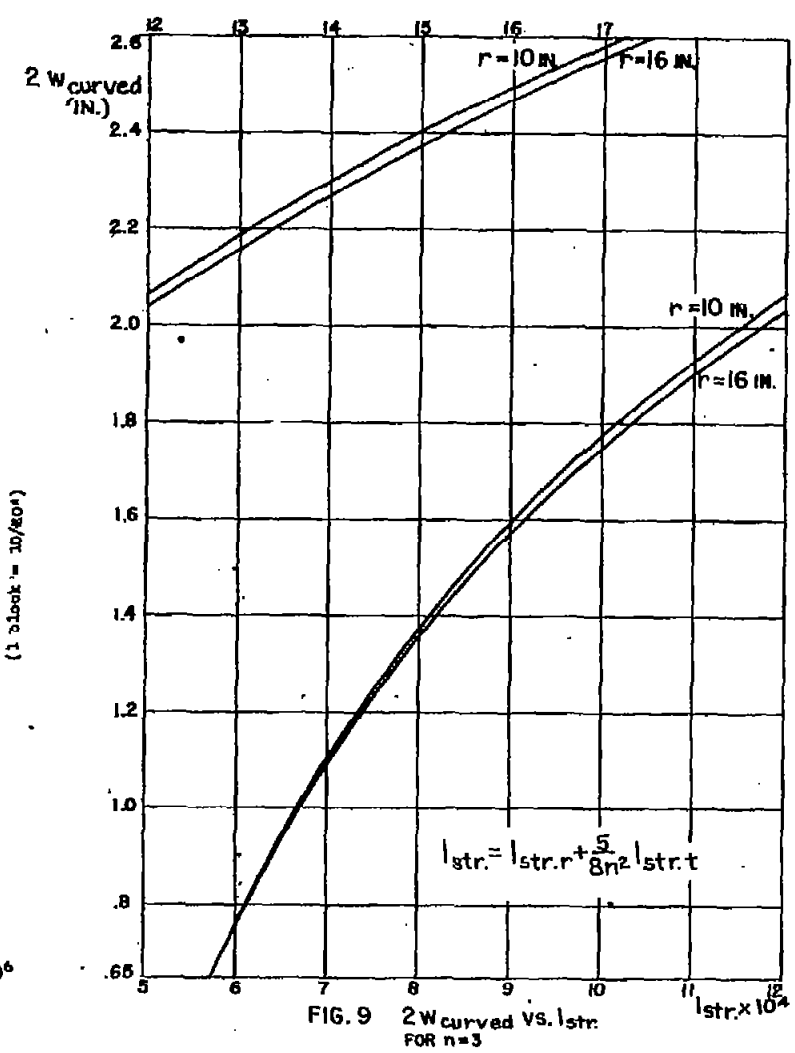

FIG. 9 $2w_{curved}$ vs. $I_{str.}$
FOR n=3

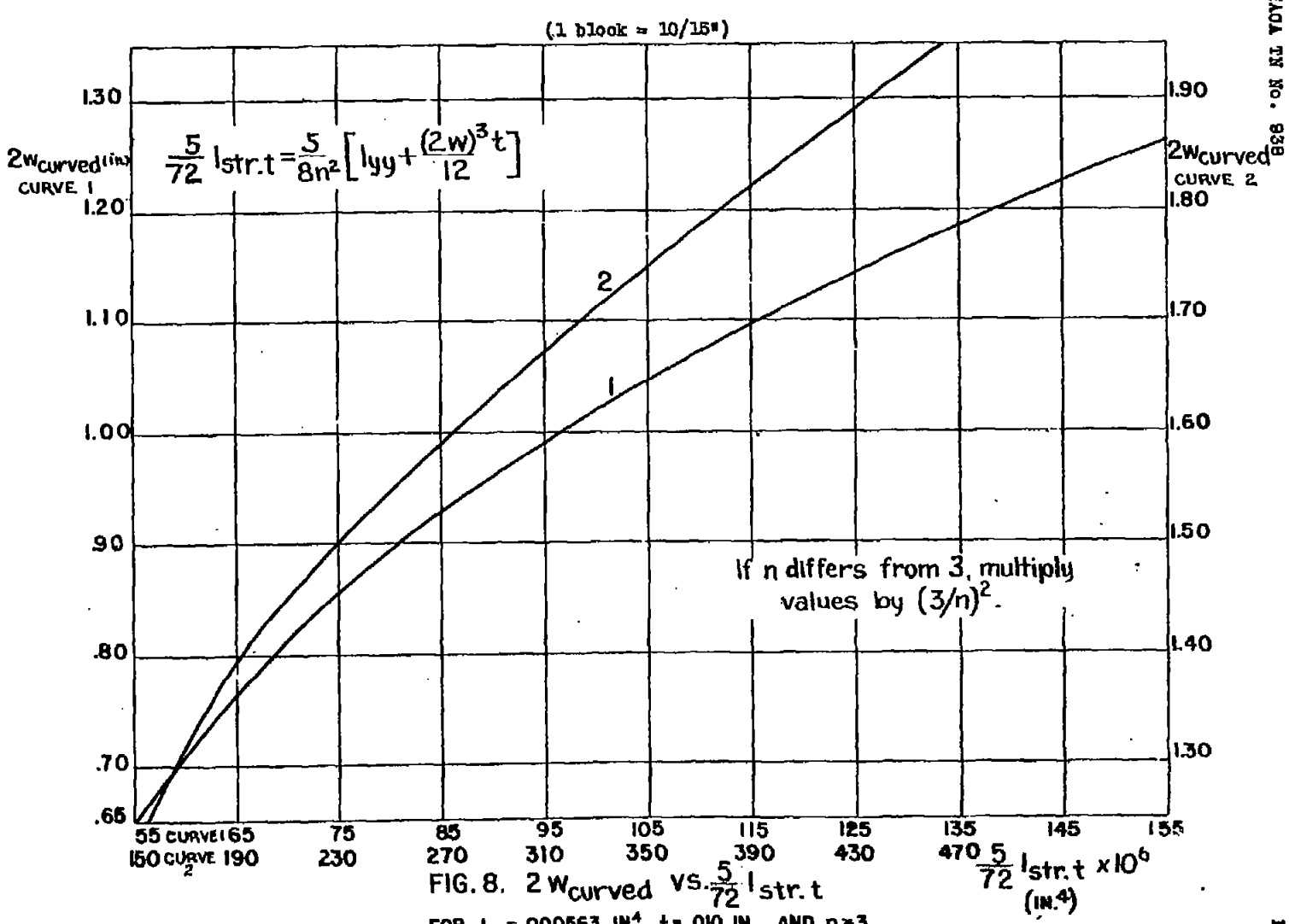

FIG. 8. $2w_{curved}$ vs. $\frac{5}{72} I_{str.t}$

FOR I_{yy}=.000563 IN.^{4}, t=.010 IN., AND n=3.

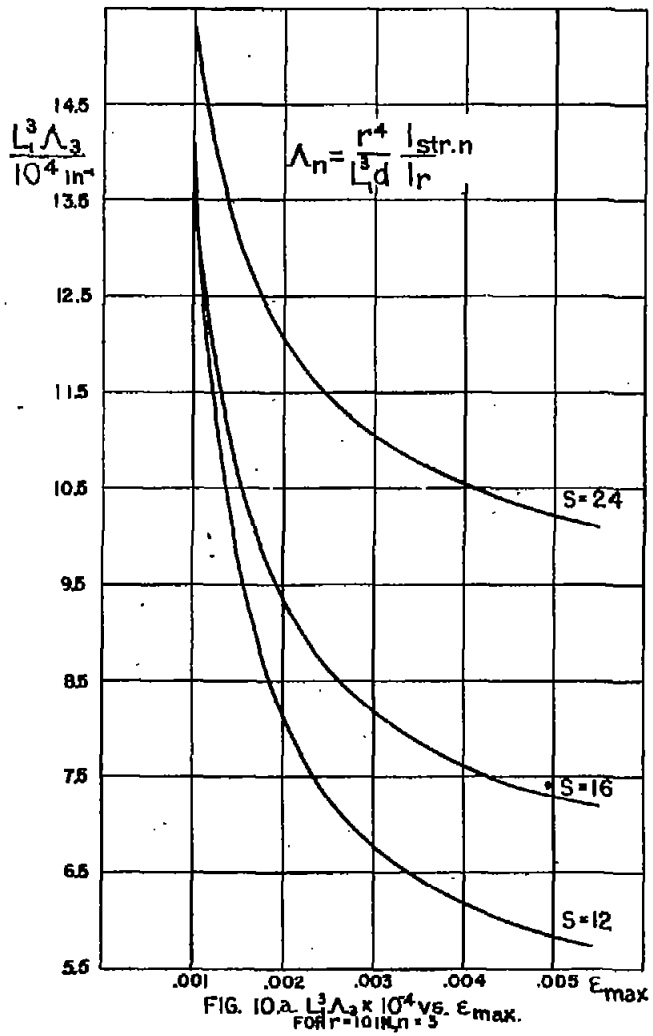

FIG. 10a $L_1^3 \Lambda_3 \times 10^4$ vs. ϵ_{max}. FOR r=10 IN., n=3

(1 block = 10/20")

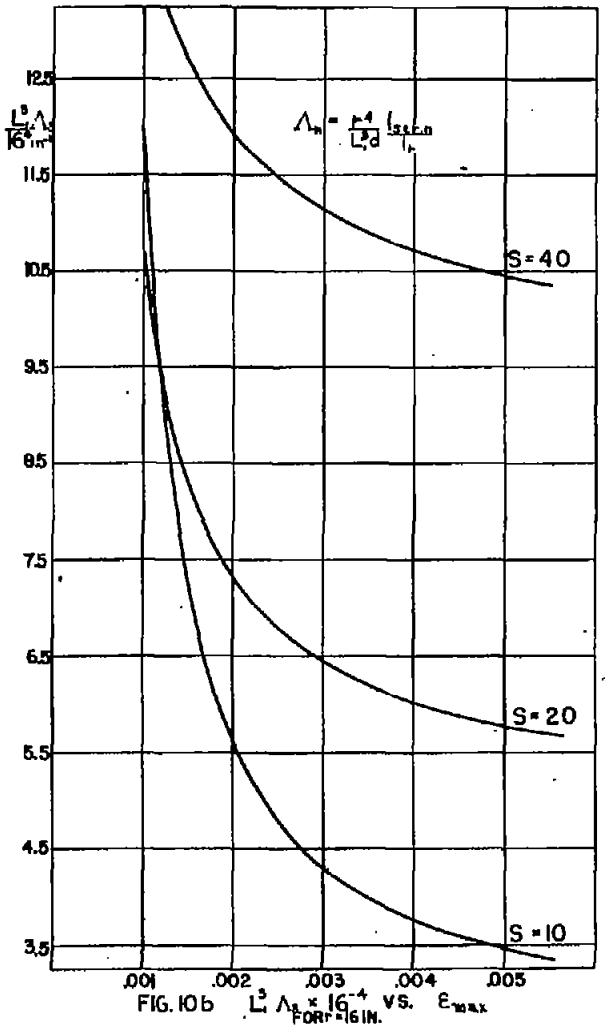

FIG. 10b $L_1^3 \Lambda_3 \times 16^{-4}$ vs. ϵ_{max} FOR r=16 IN.

Fig. 10

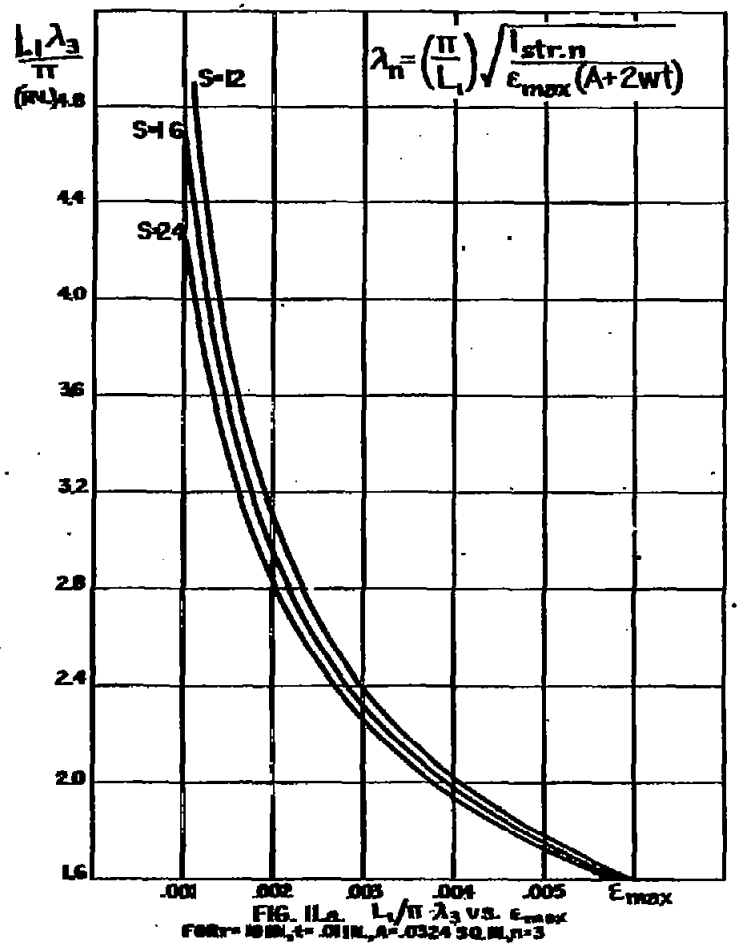

FIG. 11a. $L_1/\pi \cdot \lambda_3$ vs. ϵ_{max}
FOR r=16 IN., t=.01 IN., A=.0324 SQ.IN., n=3

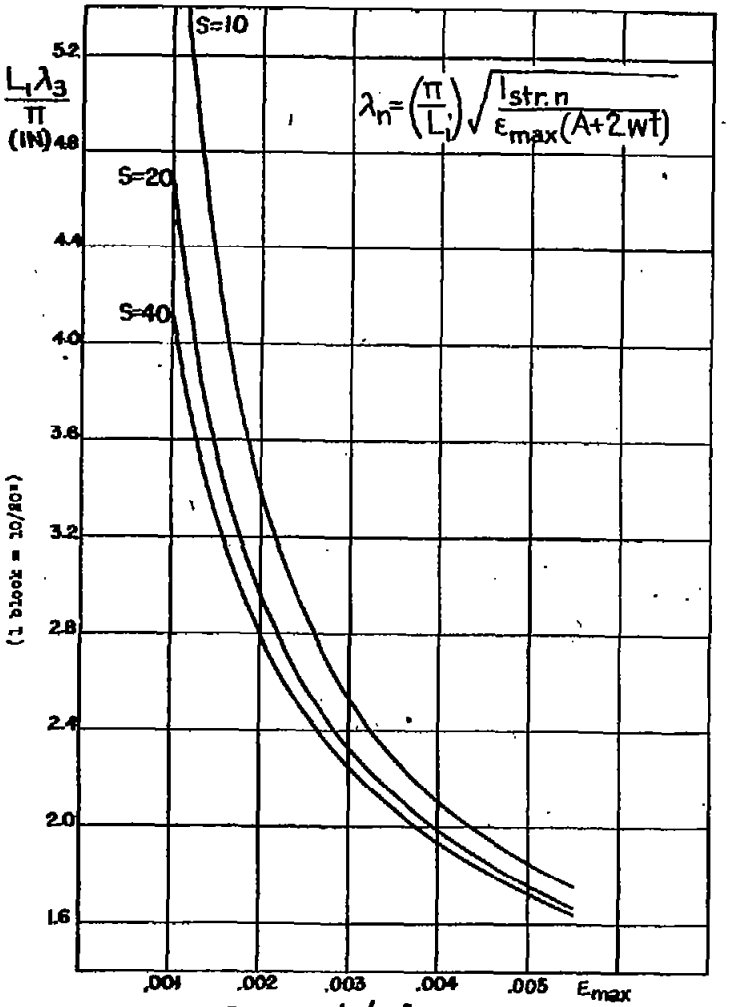

FIG. 11b. $L_1/\pi \cdot \lambda_3$ vs. ϵ_{max}
FOR r=16 IN., A=.0324 SQ.IN., t=.01 IN.
n=3

Fig. 11

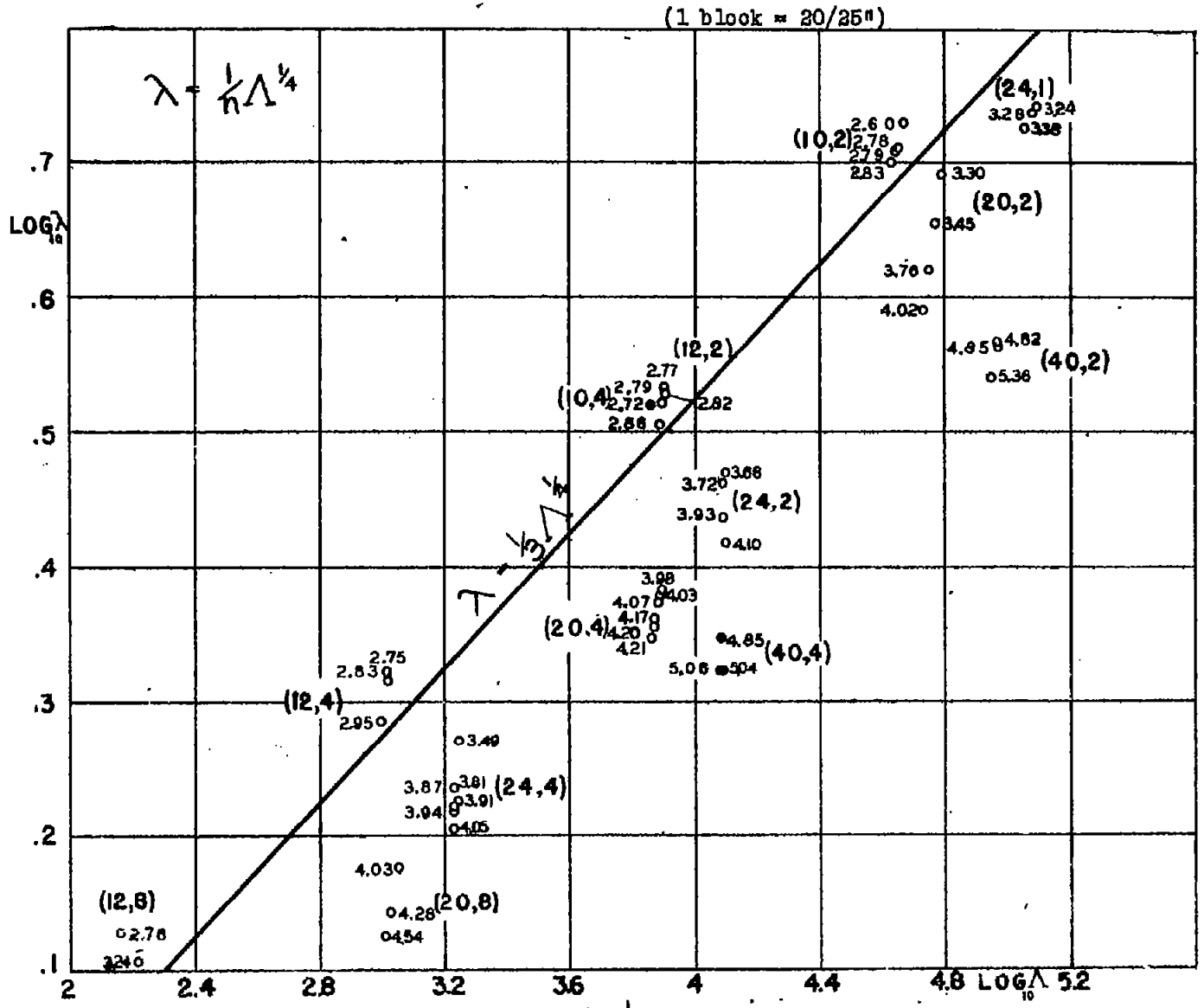

FIG. 12 $\frac{1}{4}$ POWER LAW

FIRST NUMBER IN PARENTHESES IS NUMBER OF STRINGERS, SECOND IS RING SPACING IN INCHES.
INDIVIDUAL NUMBERS REPRESENT VALUES OF n CALCULATED FROM EXPERIMENT.

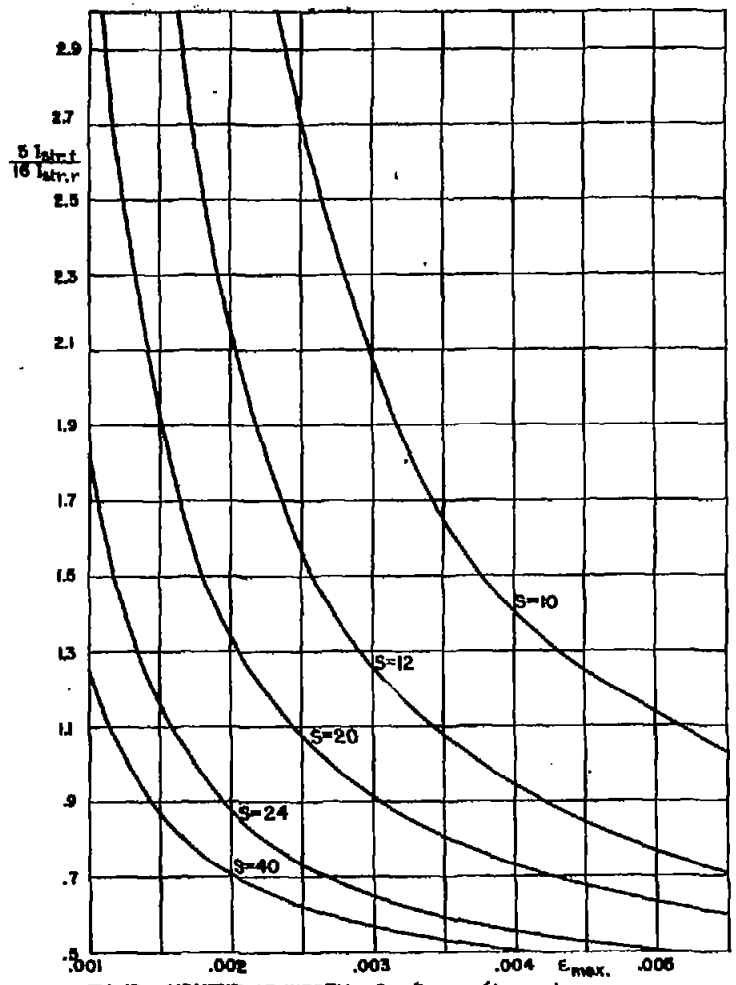

FIG. 13a. MOMENT OF INERTIA RATIO $\frac{5}{16}(I_{str.t}/I_{str.r})$ vs. $\epsilon_{max.}$

(1 block = 10/25")

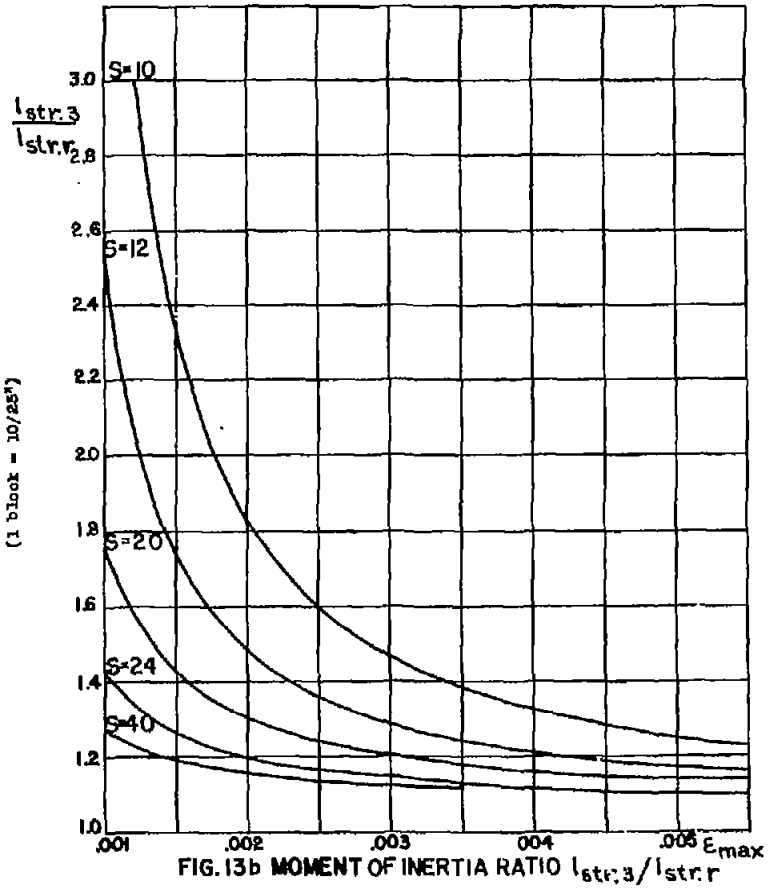

FIG. 13b MOMENT OF INERTIA RATIO $I_{str.3}/I_{str.r}$

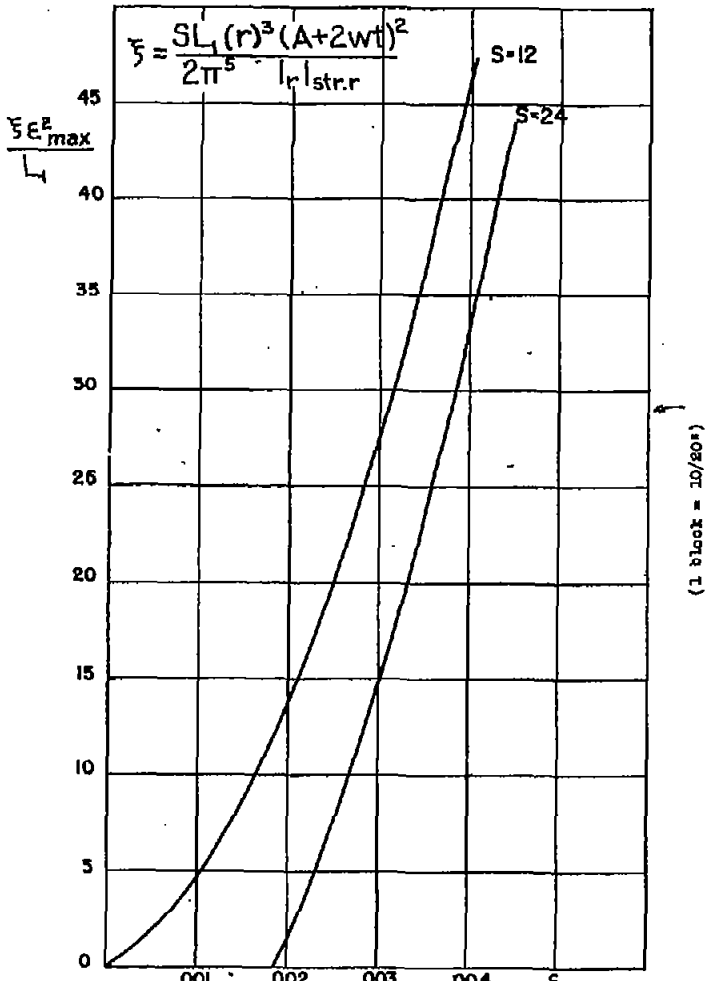

FIG. 14 $\xi \epsilon^2_{max}/L_1$ VS. ϵ_{max} FOR r= 10 IN., A = .0324 SQ. IN., t = .011 IN.

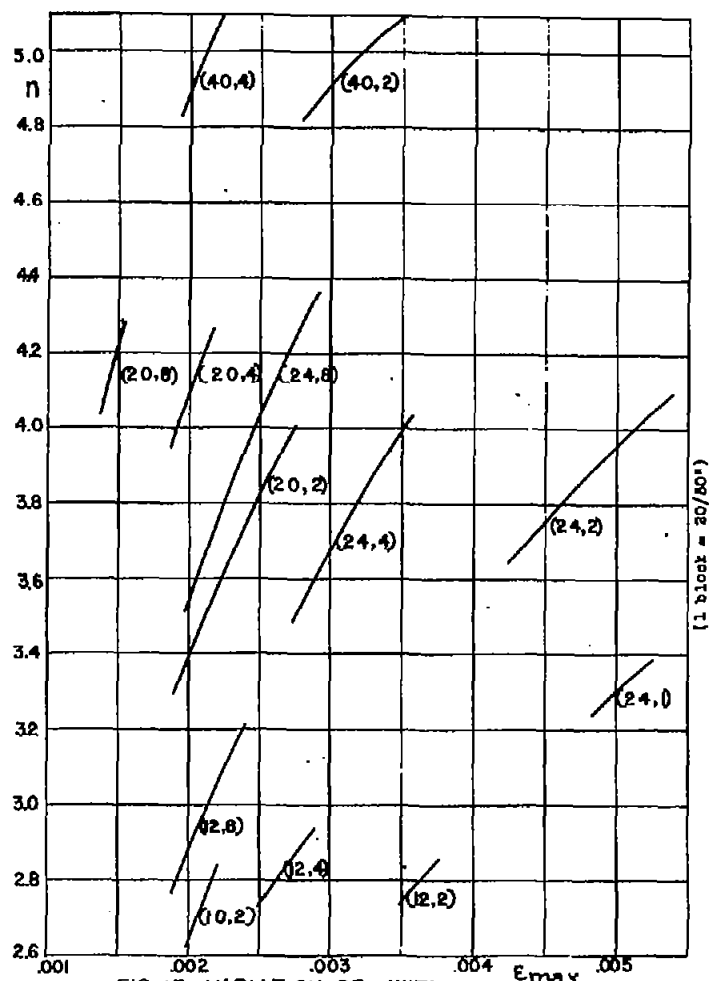

FIG. 15 VARIATION OF n WITH ϵ_{max}
FIRST NUMBER IN PARENTHESES IS NUMBER OF STRINGERS, SECOND IS RING SPACING IN INCHES.

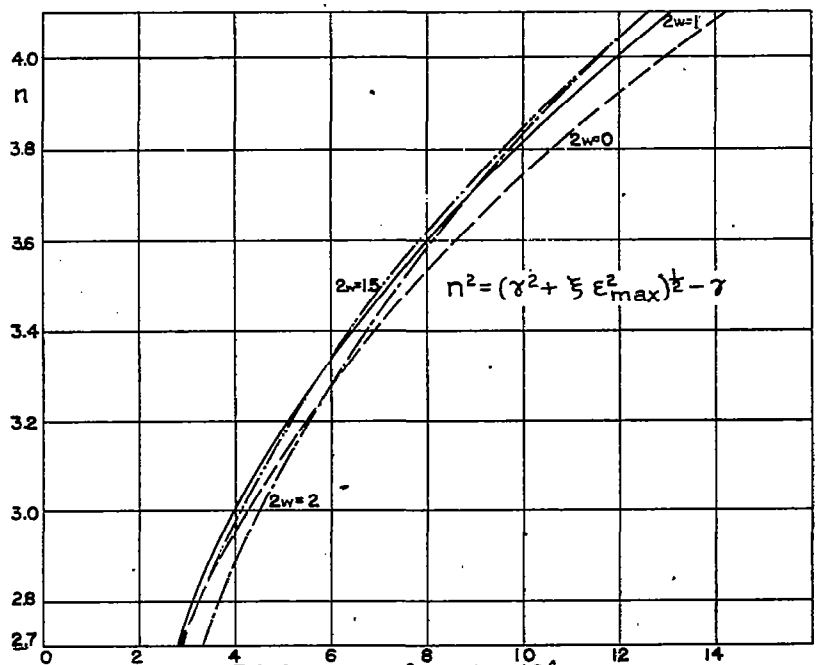

FIG. 16 n vs. ϵ^2_{max} $SL_1 \times 10^4$ (IN.) FOR r=10 IN.

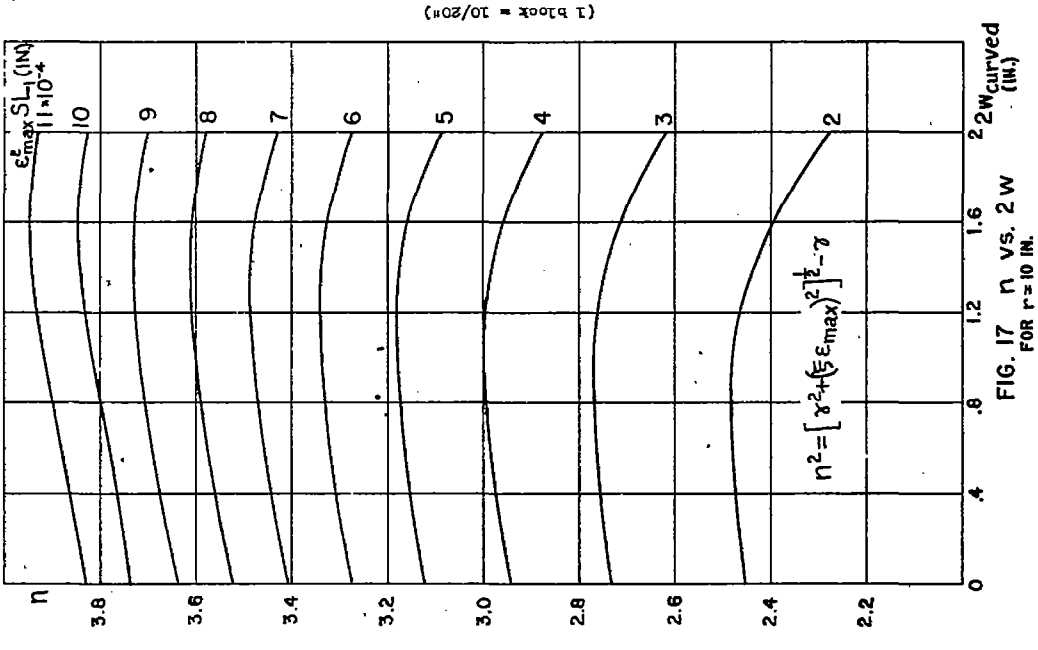

FIG. 17 n vs. 2w FOR r=10 IN.

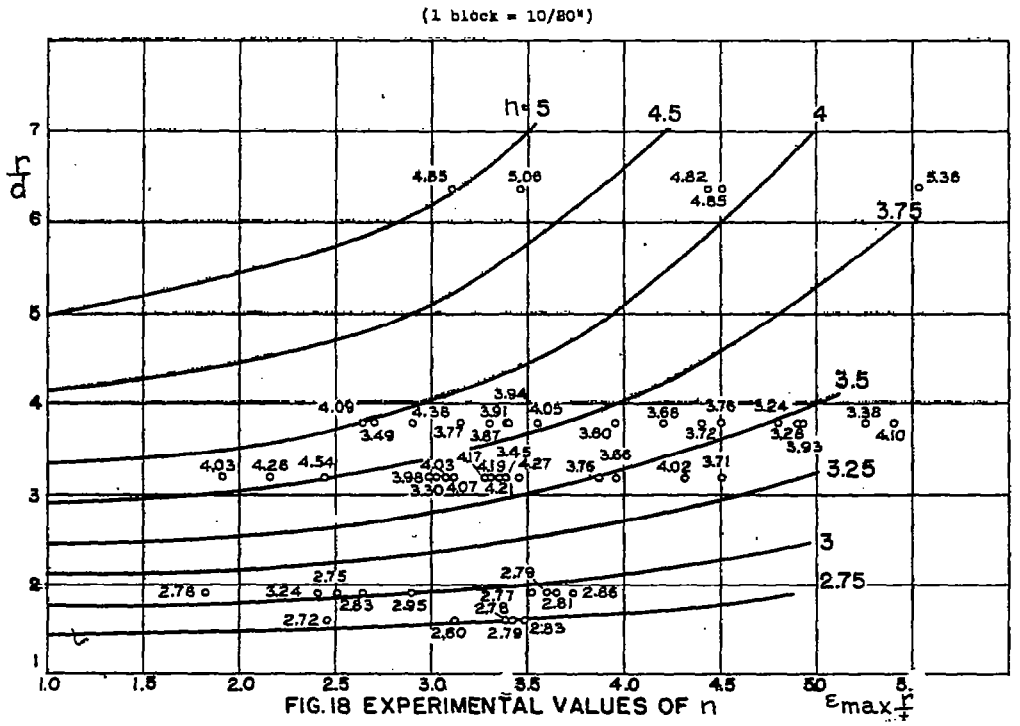

FIG. 18 EXPERIMENTAL VALUES OF n

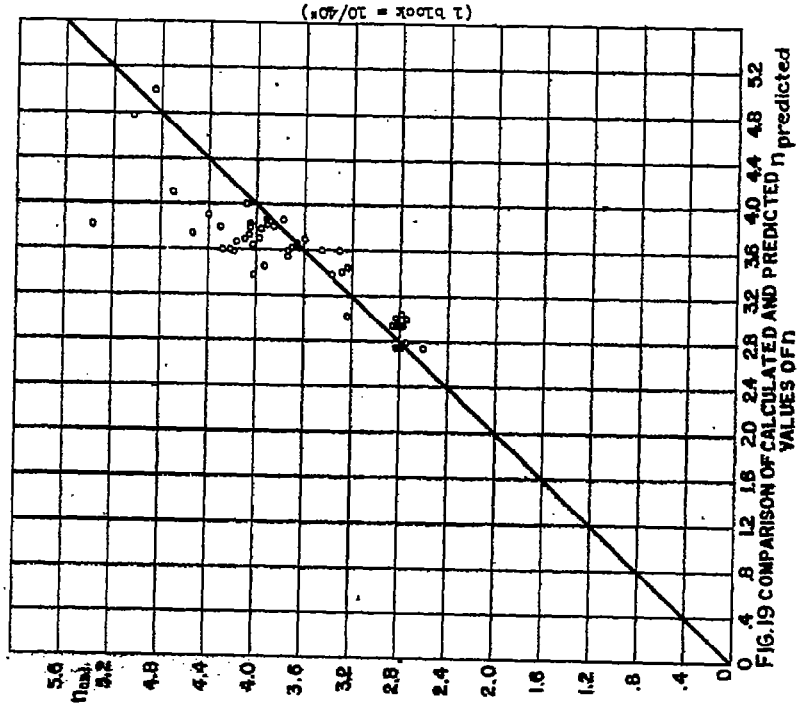

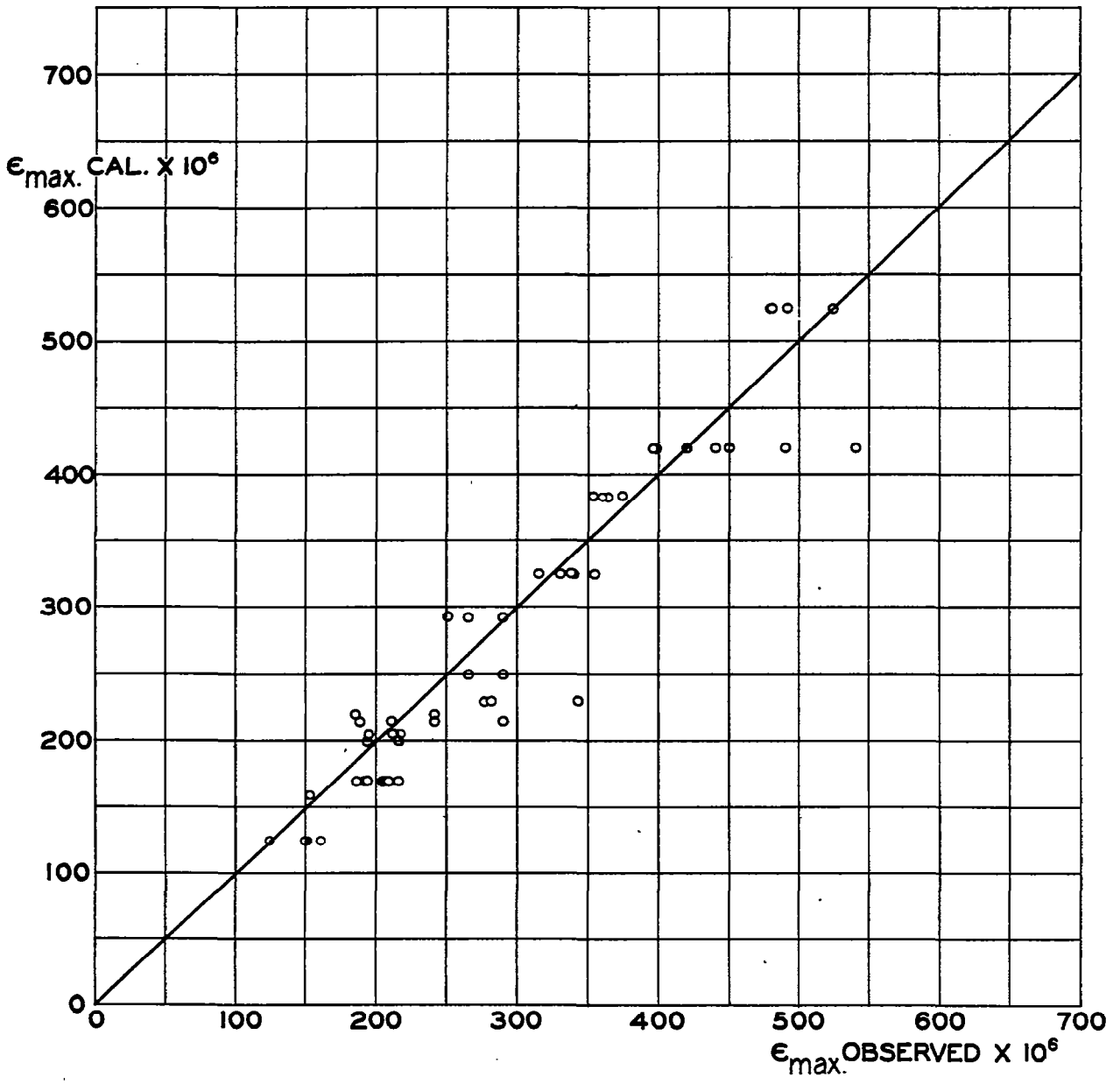

FIG. 20.- COMPARISON OF CALCULATED AND OBSERVED CRITICAL STRAIN.